Effect of a single amino acid substitution with D-amino acid within an epitope peptide, P18-I10, on LINE-IIIB recognition

Second, to examine the effect of amino acid substitution with the same weight and charged D-amino acid on LINE-IIIB recognition, a series of P18-I10-derived peptides with a single amino acid substitution by D-amino acid at each corresponding site represented by small letters in Table 1 has also been synthesized. When the corresponding D-amino acid was substituted at position 324, 325, 326, or 327, the cytotoxic activity of LINE-IIIB was markedly reduced when compared with other substituted peptides (Fig. 2). This finding suggests that CTL-TCRs can strictly recognize each amino acid within the C-terminal half of the epitope peptide, including at position 325, which is critical for determining epitope specificity, and this is in contrast to their poor ability to recognize each amino acid within the N-terminal half.

Induction of CTL line and clones specific for L-valine or D-valine at position 325 within P18-I10

Then, to study the detailed molecular interactions in determining T-cell specificity, we attempted to generate a CTL line specific for I10(325v) having a single D-type amino acid substitution in P18-I10 at position 325 using immunization of BALB/c mice with syngeneic splenic dendritic cells pulsed with the peptide (23). The I10(325v)-specific CTL line, LINE-IIIB(325D), was successfully established. Although LINE-IIIB(325D) showed some cross-reactivity to P18-I10 in a dose-dependent manner, it was highly specific for I10(325v) (Fig. 3 *A*). Similarly, LINE-IIIB had some cross-reactivity to I10(325v)-sensitized targets (Fig. 3 *B*).

Using limiting dilution techniques described elsewhere (17), we successfully established two clones, IIE11(D) and IIA4(D), predominantly specific for I10(325v) but not for P18-I10 from LINE-IIIB(325D) cells (Fig. 3 *C*) as well as two P18-I10-specific CTL clones, IIH7(L) and IB9(L), from the LINE-IIIB cells (Fig. 3 *D*). Thus, we had established four highly specific clones, two of which were specific for the D-type of valine (v), and the other two for the L-type of valine (V) at position 325 within P18-I10.

Specificity and characterization of the established CTL clones

We further examined the fine specificities of the CTL clones using a series of substituted peptides, each with a single amino acid substitution of either the L- or D-type having an aliphatic or aromatic structure at position 325 in P18-I10 (Table 1).

Among the D-specific clones, IIE11(D) did not cross-react with I10(325I) at all and was strictly specific for the D-type

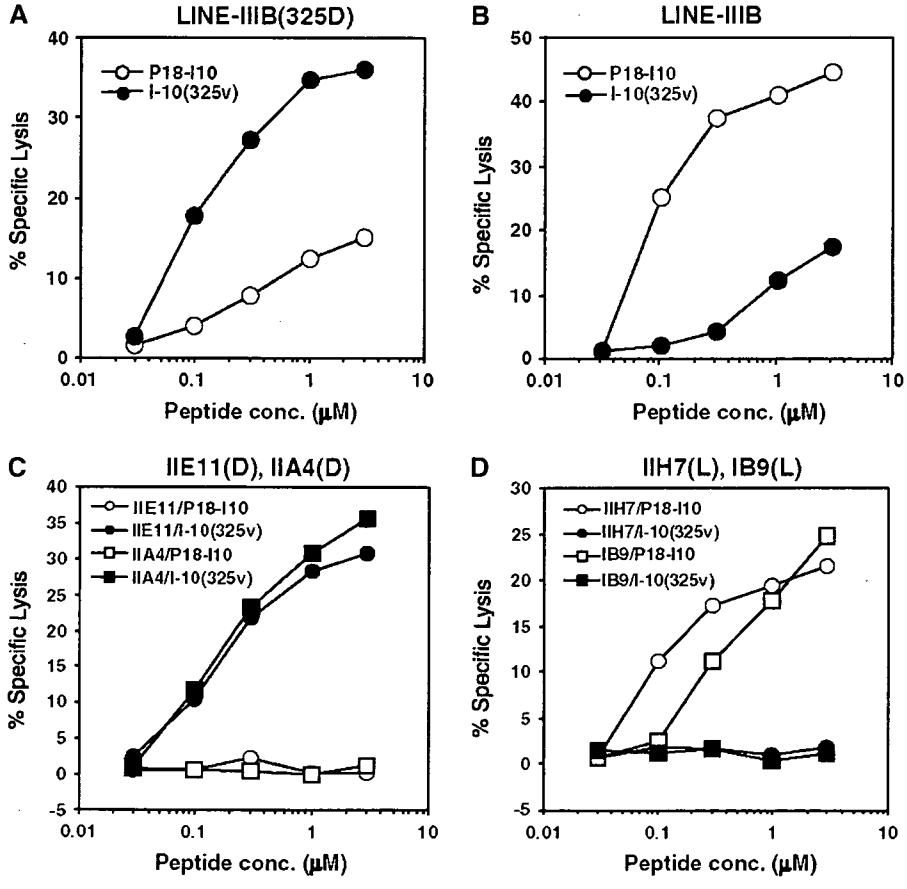

FIGURE 3 Comparison of specificity of the newly established CTL lines and clones against two peptides, peptide P18-I10 and I10(325v). We examined the cytolytic activity of the following distinct CTL lines and clones using a 5-h ^{51}Cr-release assay. To test the peptide specificity, effector cells and ^{51}Cr-labeled BALB/c.3T3 fibroblast targets (E/T ratio was 10:1) were incubated in the presence of various concentrations of either P18-I10 or I10(325v). (*A*) LINE-IIIB(325D) specific for I10(325v) was used for effector cells. (*B*) LINE-IIIB specific for P18-I10 was used for effector cells. (*C*) The CTL clones, IIE11(D) and IIA4(D), derived from LINE-IIIB(325D) were used as effector cells. (*D*) The CTL clones, IIH7(L) and IB9(L), from LINE-IIIB were used as effector cells. Standard errors of the means of triplicate cultures were <5% of the mean in each case. Each experiment was performed at least three times.

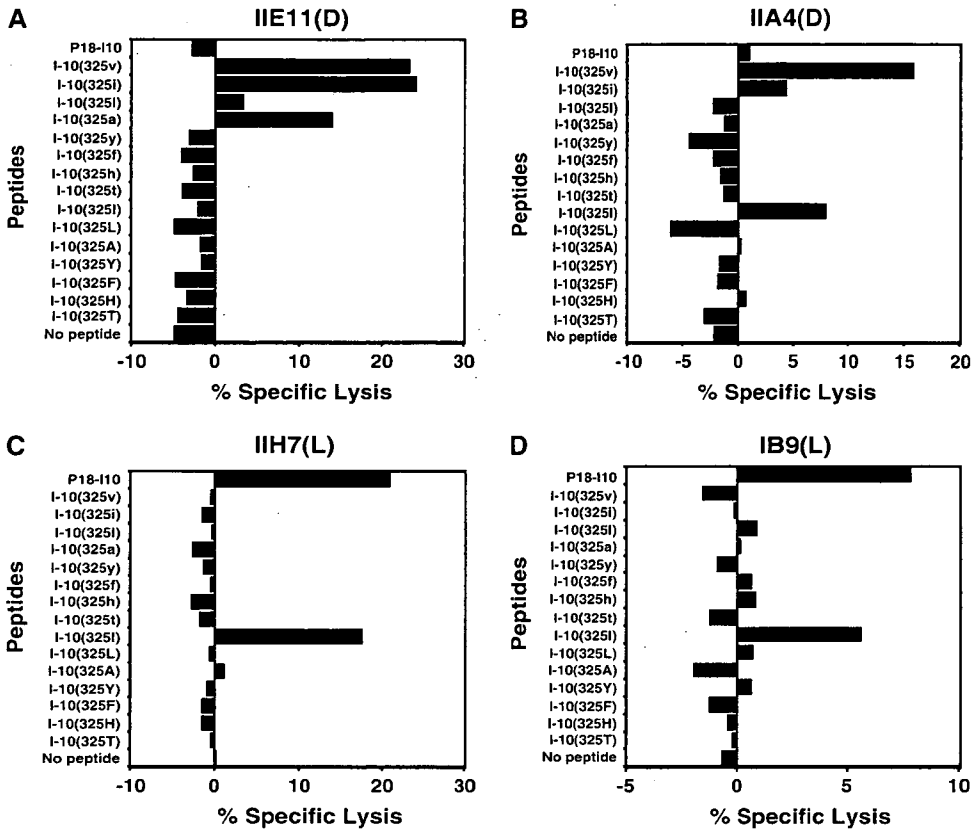

FIGURE 4 Effects of a single amino acid substitution at position 325 within P18-I10 on target sensitization for CTL recognition. We measured the cytolytic activity of the CTL lines and clones using a 5-h ^{51}Cr-release assay. For the analysis of fine peptide specificity, effector cells and ^{51}Cr-labeled BALB/c.3T3 fibroblast targets were mixed with 10 μM of each substituted peptide. The following four clones were used as effectors (E/T ratio was 20:1): (*A*) clone IIE11(D), (*B*) clone IIA4(D), (*C*) clone IIH7(L), and (*D*) clone IB9(L). Standard errors of the means of triplicate cultures were <5% of the mean in each case. Each experiment was performed at least three times.

substitution such as I10(325i) and I10(325a) as well as for the original I10(325v) (Fig. 4 *A*), whereas IIA4(D) showed a weak cross-reactivity for both types of isoleucine, I10(325I) and I10(325i), as well as for the original I10(325v) (Fig. 4 *B*). In addition, both of the L-type-specific CTL clones, IIH7(L) and IB9(L), cross-reacted with I10(325I) as well as with the original P18-I10 (Fig. 4, *C* and *D*). These findings indicate that the CTL clones can specifically distinguish the optical isomers at position 325.

Because P18-I10-specific CTL and their clones are CD8$^+$, D^d-class I MHC molecule-restricted conventional $\alpha\beta$T lymphocytes, we next confirmed the surface molecules and MHC-restriction of the I10(325v)-specific line and clones. LINE-IIIB(325D) and two clones, IIE11(D) and IIA4(D), were all CD3$^+$, CD4$^-$, CD8$^+$, and TCR$\alpha\beta^+$ by FACS analysis (data not shown), and they did not show any cytotoxicity against NK-sensitive YAC-1 cells (data not shown). Moreover, using three L cell (H-2^k) transfectants expressing the class I MHC of the d-haplotype, T4.8.3 (D^d), T1.1.1 (L^d), and B4III2 (K^d) (25,26), we confirmed that the I10(325v)-specific CTL line and clones were restricted by the D^d class I MHC molecule (data not shown).

TCR-sequences of the established clones

Taken together, the two groups of CTL clones with high specificity to the substituted P18-I10-derived peptides, having either the L-type of valine (V) or D-type of valine (v) at position 325, expressed both CD8 and $\alpha\beta$ TCRs, and were restricted by the same class I MHC molecule, D^d. Therefore, taking advantage of the unique combinations of CTL clones, we attempted to perform a precise analysis of the interaction between the TCRs of those clones and the amino acid at

	TCRα chain			
CTL clones	Vα	N	Jα	
IIE11(D)	CAMR	EAD	SNYQLIWGSGTKLIIKPD	Vα16-Jα18BBM142
IIA4(D)	CAMR	EAD	SNYQLIWGSGTKLIIKPD	Vα16-Jα18BBM142
IIH7(L)	CALS	ED	SNYQLIWGSGTKLIIKPD	Vα3-Jα18BBM142
IB9(L)	CAAS	D	SNYQLIWGSGTKLIIKPD	Vα2-Jα18BBM142

	TCRβ chain			
CTL clones	Vβ	N-D-N	Jβ	
IIE11(D)	CASS	DWGGS	TGQLYFGEGSKLTVL	Vβ8.3-Jβ2.2
IIA4(D)	CASS	DWGGS	TGQLYFGEGSKLTVL	Vβ8.3-Jβ2.2
IIH7(L)	CASS	LGYT	EVFFGKGTRLTVV	Vβ7-Jβ1.1
IB9(L)	CASS	LGVT	EVFFGKGTRLTVV	Vβ7-Jβ1.1

FIGURE 5 Nucleotide and amino acid sequences that form the V(D)J region of the TCRα and -β chain from the established CTL clones. We analyzed the amino acid sequences of TCRs in two groups of CTL clones with high specificity to substituted P18-I10-derived peptides, having either the D-type of valine (v) (IIE11(D) and IIA4(D)) or the L-type of valine (V) at position 325 (IIH7(L) and IB9(L)) restricted by the same class I MHC molecules, D^d.

position 325 within epitope to determine the specificity by comparing their TCR sequences.

To investigate the actual amino acid sequences of the TCRs in the CTL clones, we extracted their mRNA and analyzed the nucleotide sequences of the α- and β-chain transcripts after a cDNA synthesis and PCR amplifications. The Vα usage of the I10(325v)-specific clones, IIE11(D) and IIA4(D), were both Vα16 (36), whereas that of the P18-I10-specific clones, IIH7(L) and IB9(L), were Vα3 (37) and Vα2 (BLASTN Accession U88296), respectively (Fig. 5). It should be noted that all of the four distinct clones used the same uncommon Jα gene segment, 18BBM142, determined from a murine alloreactive T-cell hybridoma specific for I-A^{bm12} (38). In contrast, the Vβ usage of the 325(v)-specific clones, IIE11(D) and IIA4(D), was Vβ8.3 (39) with the Jβ 2.2 segment (40) bearing the same CDR3, "DWGGS," whereas the Vβ usage of the 325(L)-specific clones, IIH7 and IB9, was Vβ7 with the Jβ1.1 segment (41) encoding a distinct sequence, "LGYT" and "LGVT," respectively, in the CDR3 flap (Fig. 5). These results strongly indicate that the TCRβ chains of those clones may be responsible for the specificity of the epitope.

Identification of the interaction site between the TCRs and a critical amino acid at position 325 to determine epitope specificity by molecular modeling analysis

Based on the above findings, we then studied the site that determines the epitope specificity of the TCRβ chain in the CTL clones using a 3D molecular modeling analysis (see Materials and Methods). We used the LIBRA software (29,42) to select five compatible templates with excellent Standardized Scores (SD value) for both Vβ7 and Vβ8.3 (Fig. 6 *A*). Fig. 6 *B* shows the alignment of the five most suitable templates for each TCR.

We then used the MODELLER software (30,31,33) to model the 3D structure of the TCR. First, to confirm the

A

Vβ7

Rk	StrC	Lsr	Lal	Rsc	SD	Rs/N	ID%
1	1a6wH	120	127	-65.6	-4.24	-0.517	22.0
2	1dn0D	217	131	-60.1	-3.73	-0.459	19.1
3	1tcrA	202	128	-58.7	-3.60	-0.459	21.1
4	1ao7D	115	124	-56.6	-3.40	-0.457	15.3
5	1kb5A	115	122	-56.4	-3.38	-0.462	23.0

Vβ8.3

Rk	StrC	Lsr	Lal	Rsc	SD	Rs/N	ID%
1	1hxmB	230	118	-58.1	-4.24	-0.492	13.6
2	1etzB	228	124	-55.4	-3.97	-0.446	12.9
3	1fo0A	114	116	-54.5	-3.88	-0.470	19.0
4	1h5bA	113	118	-53.5	-3.78	-0.453	25.4
5	1d1fL	108	114	-52.6	-3.69	-0.461	19.3

B

Vβ7

```
          1234567890 1234567890 1234567890 1234567890 1234567890 1234567890 1234567890 1234567890
Vβ7  :  PLGTGLVDMK VTQMPRYLIK RMGENVLLEC G-QDNSHETM Y--WYRQDPG LGLQLI-YIS YDVDSNSEGD IPK-GYRVSR
1a6wH:  -------QVQ LQQPGAELVK P-GASVKLSC KASGYTFTSY WMHWVKQRPG RGLEWIGRID PNSGGTKYNE KFKSKATLTV
1dn0D:  -------EVQ LQQWGAGLLK P-SETLSLTC AVYGGSFSDY YWSWIRQPPG KGLEWIGEIN -HSGSTNYNP SLKSRVTISV
1tcrA:  --------QS VTQPDARVTV SEGASLQLRC KYSYSATPYL F--WYVQYPR QGLQLL--LK YYS-GDPVVQ GVN-GFEASF
1ao7D:  --------KE VEQNSGPLSV PEGAIASLNC TYSDRGSQSF F--WYRQYSG KSPELI--MS IYSNGDK-ED G---RFTAQL
1kb5A:  --------QQ VRQSPQSLTV WEGETAILNC SYEDSTFNYF P--WYQQFPG EGPALL--IS IRSVSDKKED G---RFTIFF

          1234567890 1234567890 1234567890 1234567890 1234567890 1234567890
          KKREH-FSLI LDSAKTNQTS VYFCASS-LG YTEVFF---G KGTRLTVVED LRNVTPPKV*
          DKPSSTAYMQ LSSLTSEDSA VYYCARYDYY GSS-YFDYWG QGTTVTVSS- ---------*
          DTSKNQFSLK LSSVTAADTA VYYCARPPHD TSGHYWNYWG QGTLVTVSSG SASA--PTL*
          SKSNSSFHLR KASVHWSDSA VYFCAVSGFA -SALTF---G SGTIVIVLPY IQNPEPA--*
          NKASQYVSLL IRDSQPSDSA TYLCAVITDS WGKLQF---G AGTQVVVTPD IQNP-----*
          NKREKKLSLH ITDSQPGDSA TYFCAARYQG GRALIF---G TGTTVSVSPG SAD------*
```

Vβ8.3

```
          1234567890 1234567890 1234567890 1234567890 1234567890 1234567890 1234567890 1234567890
Vβ8.3:  MEAAVTQSPR NKVTVTGGNV TLSCR----Q TNSHNY-MYW YRQDT-GHGL RLIHY-SYGA GNLQIGDVPD GYKATRT-TQ
1hxmB:  -AGHLEQPQI SSTKTLSKTA RLECVVSG-- ITISATSVYW YRERPGEVIQ FLVSISYDGT VRKESGIPSG KFEVDRIPET
1etzB:  -QVTLKESGP GI-LQPSQTL SLTCSFSGFS LSTSGMGVGW IRQPSGEGLE WLADIWWNDE KYYNPSLKS- RLTVSKDTSS
1fo0A:  --K-VTQTQT SISVMEKTTV TMDCV---YE TQDSSYFLFW YKQTASGEIV FLIRQDSYKK ENATVGHYSL NFQKPKS-SI
1h5bA:  GDQ-VEQSPS ALSLHEGTDS ALRCN---FT TTMRS--VQW FRQNSRGSLI SLFYLASGTK ENGRL-KSAF DSERARY-ST
1d1fL:  -DVVMTQTPL SLPVSLGNQA SISCRSS--- -SNGNTYLHW YLQKPGQSPK LLI---YKVS NRF-SGVPD- RF--SGSGSG

          1234567890 1234567890 1234567890 1234567890 1234567890
          EDFFLLLELA SPSQTSLYFC AS-SDWGGST GQL-YFGEGS KLTVL-*
          STSTLTIHNV EKQDIATYYC ALWEAQQELG KKIKVFGPGT KLI*
          NQVFLKITSV DTSDTATYHC ARRTFSYYYG SSFYYFDNWG QGTTLT*
          G---LIITAT QIEDSAVYFC AMRGDYGGSG NKL-IFGTGT LLSVE-*
          ----LHIRDA QLEDSGTYFC AAEASSGSW- -QL-IFGSGT QLTVM-*
          TDFTLKISRV EAEDLGVYFC S-----QSTH VPFT-FGSGT KLEIKR*
```

FIGURE 6 (*A*) Compatible templates with excellent Standardized Scores (SD value) for both Vβ7 and Vβ8.3 selected from the LIBRA software. Bold abbreviations are defined as follows: Rk, rank position; StrC, structural code of PDB (the last character is a subunit name); Lsr, length of the structural template; Lal, length of the aligned region; Rsc, raw score of the structural template; SD, standardized score; Rs/N, raw score (Rsc) normalized by the alignment length (Lal); ID%, sequence identity. (*B*) Sequence alignment of TCR Vβ7, Vβ8.3, and each of the five template proteins (1a6wH, 1dn0D, 1tcrA, 1ao7D, 1kb5A for Vβ7 and 1hxmB, 1etzB, 1fo0A, 1h5bA, 1d1fL for Vβ8.3) obtained from the LIBRA software. In this figure, the amino acid sequences of CDR1 and CDR3 from TCR Vβ7 or Vβ8.3 are drawn in red and green, respectively. In 10 template proteins, the corresponding portion of the CDR1 and CDR3 regions are also drawn in red and green, respectively. Conserved cysteine residues upstream of CDR1 and CDR3 are drawn in magenta. Two or three amino acids between the conserved cysteine residues and CDR1 are drawn in blue (see Discussion).

accuracy of our molecular modeling method, we predicted the 3D structure of a previously analyzed protein using MODELLER and then compared it with the experimental 3D structure obtained from x-ray crystallographic analysis for the same protein. We selected two proteins (PDB cord 1dn0D and 1a6wH) having high scores in Fig. 6 *A* and then calculated the 3D structure of 1dn0D using 1a6wH as a template. As shown in Fig. 7, the 3D structure of 1dn0D obtained from MODELLER was similar to that obtained experimentally, and their core regions were nearly identical. These results suggest that our molecular modeling method could be useful for the structural analysis of unknown TCRs.

We next predicted the 3D structures of TCR Vβ7 and Vβ8.3 and analyzed their interactions with P18-I10. The obtained 3D structures for Vβ7 using the five selected templates were quite similar (Fig. 8, *A–D*) and could be confirmed by rotating the calculated structures from various angles (data not shown). In addition, each obtained 3D structure for Vβ7 was fitted to the TCRβ part in 1kj2 to analyze the interaction with the P18-I10 peptide. Although both the CDR1 (*blue*) and CDR3 (*red*) in Vβ7 appeared to interact with the C-terminal half of P18-I10, the critical site for determining epitope specificity (325V, *bright green*) within P18-I10 was found to be more closely associated with the canonical free bottom portion of CDR1 and not with the CDR3 loop (Fig. 8, *A* and *B*): the CDR3 loop is too far from 325V. However, when the 325V was substituted with 325v (*bright red*), the CDR1 loop of Vβ7 might come in contact with the 325v (Fig. 8, *C* and *D*), which seemed to induce conformational interference between the TCR and I10(325v), and thus, the H-2D^d-restricted peptide I10(325v) would not be recognized by the P18-I10-specific clones, IIH7(L) and IB9(L). These results are consistent with our experimental results and indicate that the CDR1 loop of TCR Vβ7 should be the key site for determining P18-I10 specificity in the interaction with the L-valine at position 325.

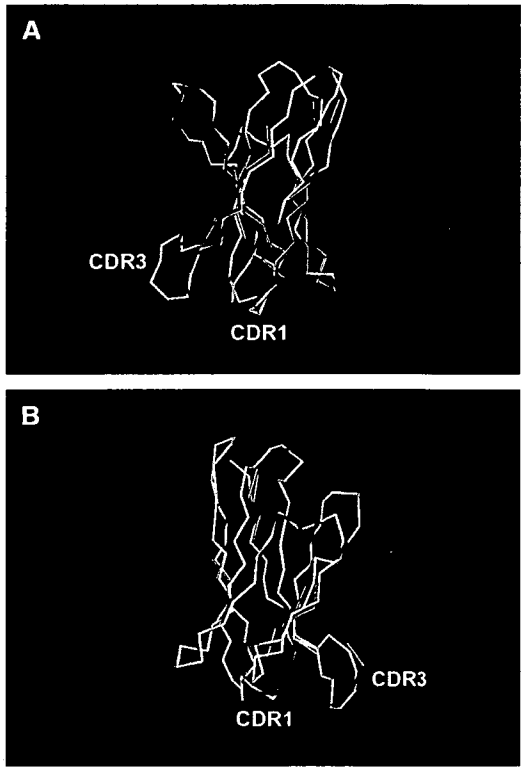

FIGURE 7 Comparison between the predicted 3D structure for 1dn0D by the MODELLER software and that of the same protein registered in PDB. The 3D structure of the protein (PDB cord 1dn0D) was predicted by the MODELLER, a molecular modeling software, using a protein (e.g., PDB cord 1a6wH) as a template. The predicted 3D structure for 1dn0D is drawn in blue, and the PDB 3D structure is drawn in red. Their backbone representations in the molecular modeling are drawn from rotated two distinct views (*A* and *B*).

Similarly, the molecular modeling for Vβ8.3 was performed using another five of the most suitable templates shown in Fig. 6 *A*; each of these actual sequences is shown in Fig. 6 *B*. The calculated 3D structures of Vβ8.3 based on the five templates had almost the same features (Fig. 8, *E–H*) as seen in the case of Vβ7. In contrast to the case of Vβ7, 325v (*bright red*) seemed to be associated with the free bottom portion of the CDR1 loop of Vβ8.3 but not with the CDR3 loop of Vβ8.3 (Fig. 8, *E* and *F*). However, the distance between the 325V (*bright green*) and the CDR1 loop in the case of Vβ8.3 appeared to be greater than that in the case of Vβ7 (Fig. 8, *G* and *H*), which can make a good contact with the 325V in P18-I10.

To substantiate the interaction between valine at position 325 and TCR-CDR1, the distance between terminal atoms in the side chain of amino acids within the epitope peptide and atoms in the main chain of the nearest portion within the TCR was calculated. As shown in Table 2, first to confirm the reliability of our molecular modeling, the distance between the two terminal atoms (OD1 and OD2) in the side chain of the seventh amino acid, aspaltic acid (D), within epitope peptide pKB1(aa: KVITFIDL) and the nearest portion in the TCR from OD1 or OD2 was determined using an already reported TCR/peptide/MHC complex, 1kj2 (PDBcode) obtained from x-ray crystallographic analysis (5). Based on the above observation, the distance between the two terminal atoms (CG1 and CG2) in the side chain of 325V or 325v and their surrounding atoms in the main chain of the obtained TCRs, Vβ7 and Vβ8.3, calculated (Tables 3 and 4) and compared with that of 1kj2. The results indicate that the distance between 325V and CDR1 in Vβ7 is similar to the distance in the case of 1kj2, whereas the distance between 325v and CDR1 in Vβ7 is too small, which may induce conformational interference between them. In contrast, the distance between 325v and CDR1 in Vβ8.3 is similar to 1kj2, but the distance between the 325V and the CDR1 in Vβ8.3 appeared to be too far from that of 1kj2. These results again agreed with our experimental results that Vβ8.3 recognized the epitope I10(325v) having D-valine at position 325 via CDR1 but did not recognize the P18-I10 containing L-valine at that position.

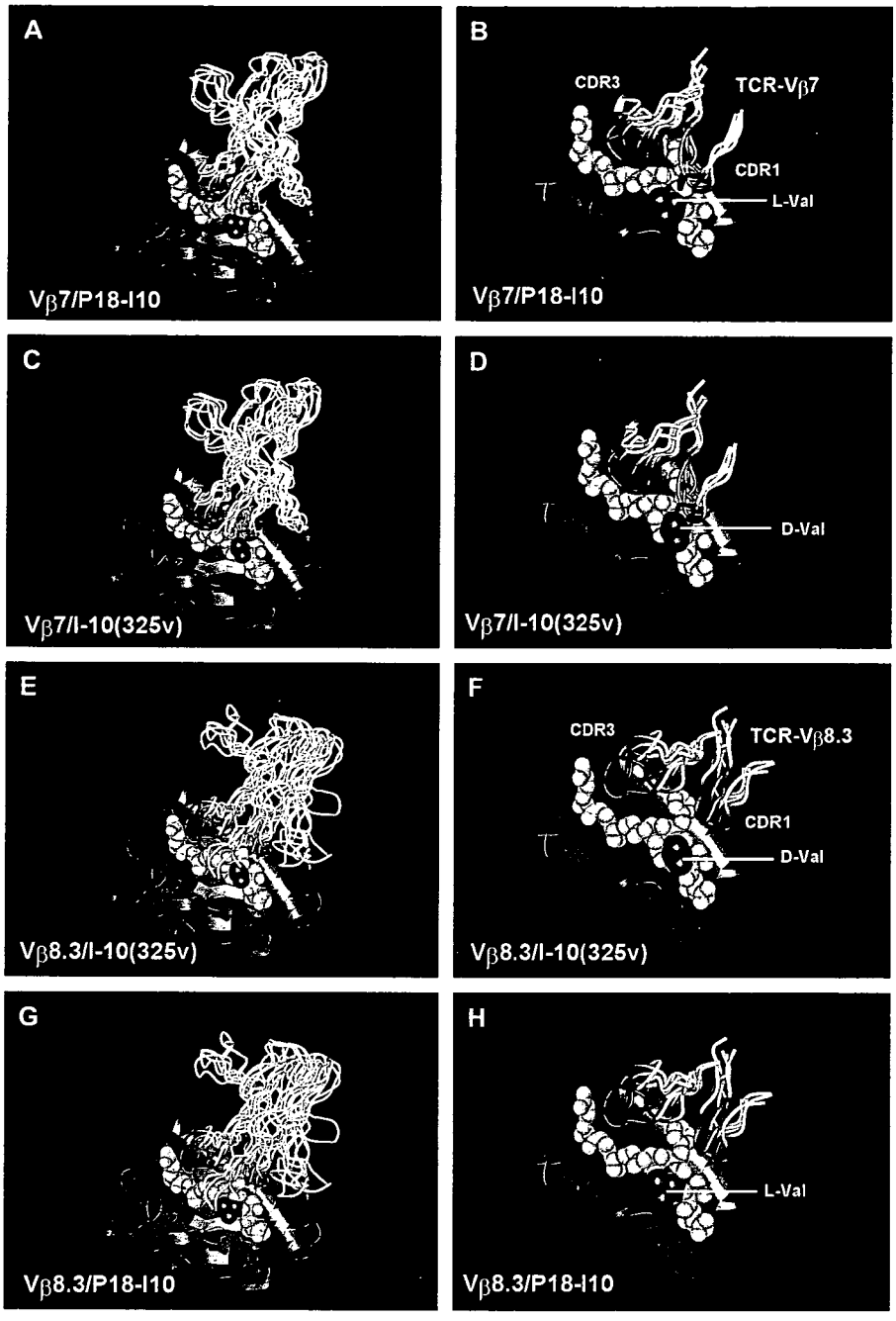

FIGURE 8 3D structures representing the interaction between TCR Vβ7 (Vβ8.3) and P18-I10/H-2D^d Complex or the interaction between TCR Vβ7 (Vβ8.3) and I10(325v)/H-2D^d complex. (*A–H*) The ternary complex of TCR Vβ7 or Vβ8.3 onto either P18-I10 or I10(325v) bounded to the H-2D^d class I MHC molecules were illustrated by computer-based molecular modeling (see Materials and Methods). Horizontal gray backbone represents the H-2D^d class I MHC molecule, and the yellow ball format indicates the D^d-bounded epitope peptide P18-I10. Vertical overlapping white backbones indicate either TCR Vβ7 or Vβ8.3. In these figures, Vβ7 and Vβ8.3 made from five distinct template proteins were overlaid in one figure. The CDR1 and CDR3 loops from both TCR Vβ chains are drawn in cyan and red, respectively. The L-type of valine (V) and the D-type of valine (v) at position 325, where epitope specificity appears to be determined, are shown in bright green and bright red, respectively. The 3D-structures of the (*A*) Vβ7 /H-2D^d/P18-I10, (*B*) enlarged figure of *A*, (*C*) Vβ7 /H-2D^d/I10(325v), (*D*) enlarged figure of *C*, (*E*) Vβ8.3 /H-2D^d/I10(325v), (*F*) enlarged figure of *E*, (*G*) Vβ8.3/H-2D^d/P18-I10, and (*H*) enlarged figure of *G* are shown in eight independent panels.

Therefore, CDR1, but not the CDR3 loop, in Vβ7 or Vβ8.3 seems to play an important role in the recognition of each specific epitope peptide. Moreover, amino acids at positions 26 to 31: DMSHET within the CDR1 of Vβ7, or TNSHNY within the CDR1 of Vβ8.3, appear to interact with the critical amino acid at position 325 to determine the epitope specificity.

DISCUSSION

In our previous study, we found that the amino acids at positions 322R and 324F were critical for D^d binding, and those at position 325V were essential for interacting with TCRs (8,17). Also, the C-terminus 327I appears to be a key amino acid for D^d binding to form the D^d-binding motif (8,18). In this study, we demonstrated that the substitution of a positively charged 322R by 322r did not result in measurable changes in target sensitization, although in our previous study the substitution with uncharged alanine (A) completely eliminated the capacity to sensitize the targets (17), indicating that a positive electric charge must be critical for D^d binding at position 322, and that a reduction of charge in the amino acid might diminish the epitope potency for T-cell activation. As shown in Fig. 1 *B*, the side chains of V and T have the same 3D

TABLE 2 The distance between two terminal atoms in the side chain of the seventh amino acid, Asp (D) within epitope peptide and atoms in main chain of the nearest portion within the TCR

	N (S28)	C_a (S28)	C (S28)	O (S28)	N (Q29)	C_a (Q29)	C (Q29)	O (Q29)	N (Y30)	C_a (Y30)	C (Y30)	O (Y30)
OD1	10.86	9.55	8.37	7.24	8.76	7.98	7.60	6.99	8.27	8.39	8.29	9.37
OD2	8.83	7.48	6.40	5.24	6.97	6.44	6.21	5.91	6.76	7.08	6.84	7.88

Unit of the distance is Å. The values are calculated using 1kj2 (PDB code), which is TCR/peptide/ MHC complex structure obtained from x-ray crystallographic analysis. The OD1 or OD2 represents the terminal atom of the side chain in the seventh amino acid, aspaltic acid (D), within epitope peptide pKB1(aa: KVITFIDL). The amino acids Ser 28 (S28), Gln 29 (Q29), and Tyr 30 (Y30) are the nearest portion within the TCR from the OD1 or OD2.

structure, except for the hydrogen atoms, if one terminal carbon atom of the side chain of V is exchanged for one oxygen atom. According to the quantum chemical calculation, the net charge of the carbon or the oxygen is −0.3e or −0.4e, respectively. In addition, three hydrogen atoms, which have positive charges, are added to the carbon, whereas one hydrogen atom is added to the oxygen. Thus, T generates a greater negative net charge than V. The influence of this charge difference was evident when LINE-IIIB recognized the peptide. It is likely that T had a greater repulsive force against the oxygen atoms in the CDR1 loop compared with V. This repulsive force may account for the significant reduction in the recognition by LINE-IIIB after substitution with T. These findings indicate that the charge of an amino acid at a specific position within an epitope can affect its binding capacity to MHC molecules and/or the interaction with a TCR.

Although the method we applied here for modeling the TCR/peptide/class I MHC complex was not directly based on crystallographic analysis, our computer-based molecular modeling was still accurate. Indeed, as demonstrated in Fig. 7, the predicted 3D structure for 1dn0D by MODELLER was similar to that determined experimentally, and the core regions appeared to be nearly identical. This reflects the fact that the 3D structures of the core regions of the TCR consist of a four-stranded antiparallel β-sheet and a three-stranded anti-parallel β-sheet linked by a disulfide bond. Although the predicted 3D structure of CDR3 seems slightly different from the experimental 3D structure of CDR3 because of the large loop, the predicted 3D structure of CDR1 appears almost the same as the experimental 3D structure. These results suggest that the TCR domain predicted by the present molecular modeling methods can become useful and reliable tools for the structural analysis of TCRs.

TABLE 3 The distance between two terminal atoms in the side chain of 325V or 325v and atoms in main chain of the obtained TCR-CDR1 through molecular modeling

	Vβ7	N(S)	Cα(S)	C(S)	O(S)	N(H)	Cα(H)	C(H)	O(H)
1a6wH	CG1(325V)	10.20	9.55	8.56	8.52	7.99	7.08	7.85	7.48
	CG2(325V)	9.57	8.88	7.62	7.41	7.01	5.80	6.17	5.57
1dn0D	CG1(325V)	10.03	9.43	8.73	8.11	9.12	8.90	9.30	9.33
	CG2(325V)	9.40	8.79	7.77	6.99	8.06	7.58	7.65	7.48
1tcrA	CG1(325V)	7.69	6.38	6.49	7.45	5.86	6.44	7.84	8.34
	CG2(325V)	6.63	5.41	5.09	5.76	4.51	4.80	6.29	6.97
1ao7D	CG1(325V)	7.57	6.48	7.18	6.85	8.40	9.21	9.59	10.11
	CG2(325V)	6.91	5.63	5.85	5.34	6.96	7.48	7.89	8.63
1kb5A	CG1(325V)	7.51	8.02	7.58	6.44	8.67	8.81	9.71	10.44
	CG2(325V)	6.77	7.06	6.21	4.99	7.08	6.92	7.89	8.79
1a6wH	CG1(325v)	8.10	7.48	6.70	6.85	6.20	5.60	6.69	6.63
	CG2(325v)	6.95	6.27	5.12	5.09	4.53	3.56	4.38	4.18
1dn0D	CG1(325v)	7.94	7.34	6.88	6.41	7.39	7.47	8.10	8.42
	CG2(325v)	6.79	6.16	5.28	4.59	5.73	5.59	5.91	6.14
1tcrA	CG1(325v)	6.51	5.12	5.35	6.50	4.59	5.40	6.57	6.84
	CG2(325v)	5.01	3.61	3.26	4.28	2.35	3.02	4.34	4.78
1ao7D	CG1(325v)	5.64	4.73	5.73	5.63	6.98	8.02	8.36	8.66
	CG2(325v)	4.39	3.09	3.63	3.36	4.88	5.73	6.12	6.61
1kb5A	CG1(325v)	5.60	6.21	6.12	5.18	7.37	7.86	8.74	9.24
	CG2(325v)	4.21	4.55	4.02	2.91	5.16	5.49	6.49	7.13

Unit of the distance is Å. The code 1a6wH, 1dn0D, 1tcrA, 1ao7D, or 1kb5A represents each template protein to determine the structure of Vβ7. CG1 and CG2 are two terminal atoms of side chain in 325V or 325v. The successive two amino acids, Ser and His, within CDR1 of Vβ7 are the nearest portion for CG1 or CG2.

In these sorts of structural analyses, it should be acknowledged that a substitution of D-valine (v) for L-valine (V) would result in a conformational interference between the class I MHC molecule and the D-valine (v), which itself could decrease the recognition response by LINE-IIIB. However, as shown in Fig. 9, no conformational interference occurred in this study. Thus, I10(325v) would also be associated with the class I MHC molecule so that TCRs may recognize the epitope. Therefore, our findings suggest that the change in the recognition response by LINE-IIIB after the D-valine (v) substitution reflects the interaction with the TCR.

Our molecular modeling analysis demonstrated that the critical area of the TCR for interacting with 325V within P18-I10 was the peptide DMSHET, within the CDR1 of Vβ7. In contrast, the substituted peptide with the D-type amino acid, I10(325v), was recognized by the peptide TNSHNY within the CDR1 of Vβ8.3. Therefore, the CDR1 in the Vβ7 or Vβ8.3 might play an important role in recognizing the epitope P18-I10 or I10(325v), respectively, and, in particular, the distance between CDR1 and the amino acid 325V or 325v within the peptide seemed to be essential for recognizing the epitope. Taken together, the results derived from our molecular modeling strategy appear to be consistent with the experimental results.

Although the epitope specificity created by TCRs has been reported to be dependent mainly on the amino acid sequences in the CDR3 regions for both the TCRα and β chains (43,44), crystallographic analyses on various TCR and peptide/MHC interactions have suggested that both the CDR1 and CDR3 in

TABLE 4 The distance between two terminal atoms in the side chain of 325V or 325v and atoms in main chain of the obtained TCR-CDR1 through molecular modeling

Vβ8.3	N(T)	Cα(T)	C(T)	O(T)	N(N)	Cα(N)	C(N)	O(N)	N(S)	Cα(S)	C(S)	O(S)
1hxmBCG1(325V)	13.34	12.22	11.94	12.32	11.47	11.47	10.62	9.61	11.19	10.74	11.80	12.32
CG2(325V)	12.54	11.59	11.25	11.41	11.00	10.98	9.90	8.83	10.34	9.64	10.65	11.36
1etzBCG1(325V)	13.77	13.45	12.19	11.26	12.24	11.31	9.99	8.95	10.16	9.20	9.41	10.25
CG2(325V)	13.14	12.75	11.63	10.76	11.76	11.02	9.57	8.73	9.41	8.22	8.32	9.30
1fo0ACG1(325V)	10.43	9.82	9.37	9.20	9.43	9.34	10.58	11.43	10.85	12.07	13.27	13.89
CG2(325V)	9.41	8.58	8.29	8.45	8.18	8.25	9.66	10.47	10.12	11.47	12.47	13.09
1h5bACG1(325V)	11.98	10.99	10.34	10.13	10.23	9.81	10.97	12.02	10.95	12.14	12.24	11.29
CG2(325V)	11.18	10.43	9.87	9.95	9.52	9.16	10.18	11.13	10.20	11.29	11.10	10.02
1dlfLCG1(325V)	12.46	11.35	10.28	9.72	10.18	9.27	10.19	11.40	9.77	10.82	11.61	11.18
CG2(325V)	11.39	10.46	9.42	9.14	9.06	8.14	9.06	10.25	8.69	9.75	10.28	9.64
1hxmBCG1(325v)	11.19	10.04	9.53	9.84	8.98	8.81	7.89	6.96	8.39	7.95	9.00	9.47
CG2(325v)	10.21	9.16	8.72	8.95	8.37	8.32	7.31	6.25	7.84	7.33	8.47	9.12
1etzBCG1(325v)	11.63	11.33	10.01	9.08	10.05	9.08	7.83	6.75	8.15	7.37	7.76	8.53
CG2(325v)	10.57	10.17	9.00	8.11	9.13	8.38	6.95	6.11	6.87	5.78	6.11	7.09
1fo0ACG1(325v)	8.55	8.16	7.68	7.31	7.99	7.98	9.10	9.82	9.44	10.57	11.78	12.26
CG2(325v)	6.96	6.31	6.03	6.03	6.22	6.47	7.78	8.44	8.38	9.66	10.67	11.12
1h5bACG1(325v)	9.98	8.91	8.17	7.84	8.17	7.74	8.99	10.05	9.05	10.33	10.63	9.80
CG2(325v)	8.70	7.89	7.22	7.27	6.92	6.57	7.69	8.66	7.83	9.04	9.03	8.07
1dlfLCG1(325v)	10.66	9.50	8.36	7.65	8.40	7.51	8.42	9.61	8.05	9.15	10.11	9.84
CG2(325v)	9.11	8.13	6.97	6.57	6.70	5.75	6.71	7.91	6.41	7.59	8.30	7.82

Unit of the distance is Å. The code 1hxmB, 1etzB, 1fo0A, 1h5bA, or 1dlfL represents each template protein to determine the structure of Vβ8.3. CG1 and CG2 are two terminal atoms of side chain in 325V or 325v. The successive three amino acids, Thr, Asn, and Ser, within CDR1 of Vβ8.3 are the nearest portion for CG1 or CG2.

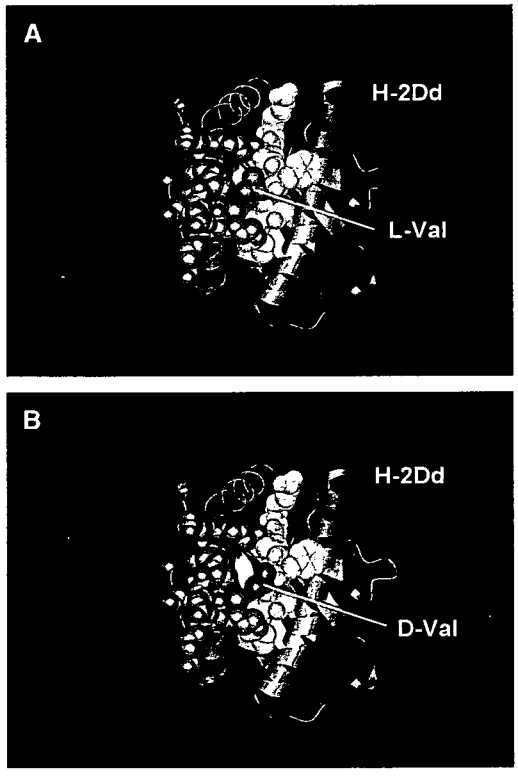

FIGURE 9 (*A* and *B*) 3D structures of P18-I10/H-2D^d complex and I10(325v)/H-2D^d complex. Gray ribbon and ball format represent the H-2D^d class I MHC molecule, and the yellow ball format indicates the D^d-bounded epitope peptide, P18-I10 or I10(325v). In the H-2D^d class I MHC molecule, only the positions for interaction with 325V are drawn in the ball format, for clarity. The L-type of valine (V) and the D-type of valine (v) at position 325 are shown in green and red, respectively. Radius of ball format indicates van der Waals radius.

the TCRα and TCRβ chains might contact with the antigenic peptide/MHC complex (1,2,5,6), particularly with the carboxyl-terminal portion of the peptides (2). Moreover, recent reports have shown that the CDR1 in Vβ10 participated in class I MHC molecule-mediated T-cell recognition (45,46). In these reports, significant alteration in the capacity to bind class I MHC molecules and in the ability to respond to the peptide/MHC complex was demonstrated when a single amino acid substitution was introduced into the CDR1 of TCR Vβ10 by site-directed mutagenesis. Indeed, we have shown here that the CDR1 in the TCRβ chains appeared to interact directly with the key amino acid for determining epitope specificity. Thus, if the most critical amino acid for determining the epitope specificity is located near the C-terminal portion of a peptide such as P18-I10, not only the CDR3 but also the CDR1 in the TCRβ chain may be involved in determining antigen specificity.

It is also important to consider the role of the primary structures in TCR recognition. As demonstrated in Fig. 6 *B*, there are two cysteine (C) residues positioned upstream of CDR1 (*magenta*) and CDR3 (*magenta*) of both TCR Vβ7 and Vβ8.3. These residues bind each other via a disulfide bond and must be a basic structure of TCRs because they are conserved in most of the murine TCR sequences (47) . The two or three amino acids (*blue*) between the conserved cysteine (C) residues and the CDR1 would be key amino acids in forming the 3D structure of CDR1, although they do not interact directly with the epitope peptide. If only these amino acids are exchanged for other amino acids, the 3D structure of CDR1 affecting the recognition of an amino acid at position 325 would change. Indeed, these amino acids are

highly variable for both TCR Vβ7 and Vβ8.3 (Fig. 6 *B*) and for various other murine TCR sequences (47), whereas the regions just after CDR1 are mostly conserved. These amino acids are likely to participate in the peptide recognition by creating small changes in the 3D structure of CDR1. In this regard, both CDR1 and the two or three amino acids between the cysteine (C) and CDR1 may play a important role in recognizing position 325 within P18-I10 or I10(325v).

We thank Dr. Megumi Takahashi for her assistance with the DNA sequence analysis of the TCRs.

This work was supported in part by grants from the Ministry of Education, Science, Sport, and Culture, from the Ministry of Health and Labor and Welfare, Japan; from the Japanese Health Sciences Foundation; and from and by the Promotion and Mutual Aid Corporation for Private Schools of Japan.

REFERENCES

1. Garboczi, D. N., P. Ghosh, U. Utz, Q. R. Fan, W. E. Biddison, and D. C. Wiley. 1996. Structure of the complex between human T-cell receptor, viral peptide and HLA-A2. *Nature.* 384:134–141.
2. Garcia, K. C., M. Degano, R. L. Stanfield, A. Brunmark, M. R. Jackson, P. A. Peterson, L. Teyton, and I. A. Wilson. 1996. An alphabeta T cell receptor structure at 2.5 A and its orientation in the TCR-MHC complex. *Science.* 274:209–219.
3. Garboczi, D. N., and W. E. Biddison. 1999. Shapes of MHC restriction. *Immunity.* 10:1–7.
4. Hennecke, J., and D. C. Wiley. 2001. T cell receptor-MHC interactions up close. *Cell.* 104:1–4.
5. Reiser, J. B., C. Gregoire, C. Darnault, T. Mosser, A. Guimezanes, A. M. Schmitt-Verhulst, J. C. Fontecilla-Camps, G. Mazza, B. Malissen, and D. Housset. 2002. A T cell receptor CDR3beta loop undergoes conformational changes of unprecedented magnitude upon binding to a peptide/MHC class I complex. *Immunity.* 16:345–354.
6. Garcia, K. C., M. Degano, L. R. Pease, M. Huang, P. A. Peterson, L. Teyton, and I. A. Wilson. 1998. Structural basis of plasticity in T cell receptor recognition of a self peptide-MHC antigen. *Science.* 279: 1166–1172.
7. Takahashi, H., J. Cohen, A. Hosmalin, K. B. Cease, R. Houghten, J. L. Cornette, C. DeLisi, B. Moss, R. N. Germain, and J. A. Berzofsky. 1988. An immunodominant epitope of the human immunodeficiency virus envelope glycoprotein gp160 recognized by class I major histocompatibility complex molecule-restricted murine cytotoxic T lymphocytes. *Proc. Natl. Acad. Sci. USA.* 85:3105–3109.
8. Takeshita, T., H. Takahashi, S. Kozlowski, J. D. Ahlers, C. D. Pendleton, R. L. Moore, Y. Nakagawa, K. Yokomuro, B. S. Fox, and D. H. Margulies. 1995. Molecular analysis of the same HIV peptide functionally binding to both a class I and a class II MHC molecule. *J. Immunol.* 154:1973–1986.
9. Takahashi, H., S. Merli, S. D. Putney, R. Houghten, B. Moss, R. N. Germain, and J. A. Berzofsky. 1989. A single amino acid interchange yields reciprocal CTL specificities for HIV-1 gp160. *Science.* 246: 118–121.
10. Takahashi, H., Y. Nakagawa, C. D. Pendleton, R. A. Houghten, K. Yokomuro, R. N. Germain, and J. A. Berzofsky. 1992. Induction of broadly cross-reactive cytotoxic T cells recognizing an HIV-1 envelope determinant. *Science.* 255:333–336.
11. Shirai, M., C. D. Pendleton, and J. A. Berzofsky. 1992. Broad recognition of cytotoxic T cell epitopes from the HIV-1 envelope protein with multiple class I histocompatibility molecules. *J. Immunol.* 148: 1657–1667.
12. Palker, T. J., M. E. Clark, A. J. Langlois, T. J. Matthews, K. J. Weinhold, R. R. Randall, D. P. Bolognesi, and B. F. Haynes. 1988. Type-specific neutralization of the human immunodeficiency virus with antibodies to env-encoded synthetic peptides. *Proc. Natl. Acad. Sci. USA.* 85:1932–1936.
13. Rusche, J. R., K. Javaherian, C. McDanal, J. Petro, D. L. Lynn, R. Grimaila, A. Langlois, R. C. Gallo, L. O. Arthur, P. J. Fischinger, D. P. Bolognesi, S. D. Putney, and T. J. Matthews 1988. Antibodies that inhibit fusion of human immunodeficiency virus-infected cells bind a 24-amino acid sequence of the viral envelope, gp120. *Proc. Natl. Acad. Sci. USA.* 85:3198–3202.
14. Goudsmit, J., C. Debouck, R. H. Meloen, L. Smit, M. Bakker, D. M. Asher, A. V. Wolff, C. J. Gibbs, Jr., and D. C. Gajdusek. 1988. Human immunodeficiency virus type 1 neutralization epitope with conserved architecture elicits early type-specific antibodies in experimentally infected chimpanzees. *Proc. Natl. Acad. Sci. USA.* 85:4478–4482.
15. Takahashi, H., R. N. Germain, B. Moss, and J. A. Berzofsky. 1990. An immunodominant class I-restricted cytotoxic T lymphocyte determinant of human immunodeficiency virus type 1 induces CD4 class II-restricted help for itself. *J. Exp. Med.* 171:571–576.
16. Clerici, M., D. R. Lucey, R. A. Zajac, R. N. Boswell, H. M. Gebel, H. Takahashi, J. A. Berzofsky, and G. M. Shearer. 1991. Detection of cytotoxic T lymphocytes specific for synthetic peptides of gp160 in HIV-seropositive individuals. *J. Immunol.* 146:2214–2219.
17. Takahashi, H., R. Houghten, S. D. Putney, D. H. Margulies, B. Moss, R. N. Germain, and J. A. Berzofsky. 1989. Structural requirements for class I MHC molecule-mediated antigen presentation and cytotoxic T cell recognition of an immunodominant determinant of the human immunodeficiency virus envelope protein. *J. Exp. Med.* 170:2023–2035.
18. Corr, M., L. F. Boyd, E. A. Padlan, and D. H. Margulies. 1993. H-2Dd exploits a four residue peptide binding motif. *J. Exp. Med.* 178:1877–1892.
19. Jorgensen, J. L., U. Esser, B. Fazekas de St Groth, P. A. Reay, and M. M. Davis. 1992. Mapping T-cell receptor-peptide contacts by variant peptide immunization of single-chain transgenics. *Nature.* 355:224–230.
20. Cease, K. B., H. Margalit, J. L. Cornette, S. D. Putney, W. G. Robey, C. Ouyang, H. Z. Streicher, P. J. Fischinger, R. C. Gallo, C. DeLisi, and J. A. Berzofsky. 1987. Helper T-cell antigenic site identification in the acquired immunodeficiency syndrome virus gp120 envelope protein and induction of immunity in mice to the native protein using a 16-residue synthetic peptide. *Proc. Natl. Acad. Sci. USA.* 84:4249–4253.
21. Boehncke, W. H., T. Takeshita, C. D. Pendleton, R. A. Houghten, S. Sadegh-Nasseri, L. Racioppi, J. A. Berzofsky, and R. N. Germain. 1993. The importance of dominant negative effects of amino acid side chain substitution in peptide-MHC molecule interactions and T cell recognition. *J. Immunol.* 150:331–341.
22. Zhang, W., S. Honda, F. Wang, T. P. DiLorenzo, A. M. Kalergis, D. A. Ostrov, and S. G. Nathenson. 2001. Immunobiological analysis of TCR single-chain transgenic mice reveals new possibilities for interaction between CDR3alpha and an antigenic peptide bound to MHC class I. *J. Immunol.* 167:4396–4404.
23. Takahashi, H., Y. Nakagawa, K. Yokomuro, and J. A. Berzofsky. 1993. Induction of $CD8^+$ cytotoxic T lymphocytes by immunization with syngeneic irradiated HIV-1 envelope derived peptide-pulsed dendritic cells. *Int. Immunol.* 5:849–857.
24. Takahashi, H., Y. Nakagawa, G. R. Leggatt, Y. Ishida, T. Saito, K. Yokomuro, and J. A. Berzofsky. 1996. Inactivation of human immunodeficiency virus (HIV)-1 envelope-specific $CD8^+$ cytotoxic T lymphocytes by free antigenic peptide: a self-veto mechanism? *J. Exp. Med.* 183:879–889.
25. Margulies, D. H., G. A. Evans, K. Ozato, R. D. Camerini-Otero, K. Tanaka, E. Appella, and J. G. Seidman. 1983. Expression of H-2Dd and H-2Ld mouse major histocompatibility antigen genes in L cells after DNA-mediated gene transfer. *J. Immunol.* 130:463–470.
26. Abastado, J.P., C. Jaulin, M.P. Schutze, P. Langlade_Demoyen, F. Plata, K. Ozato, and P. Kourilsky. 1987. Fine mapping of epitopes by intradomain K^d/D^d recombinants. *J. Exp. Med.* 166:327–340.
27. Takahashi, M., E. Osono, Y. Nakagawa, J. Wang, J. A. Berzofsky, D. H. Margulies, and H. Takahashi. 2002. Rapid induction of apoptosis in $CD8^+$ HIV-1 envelope-specific murine CTLs by short exposure to antigenic peptide. *J. Immunol.* 169:6588–6593.

28. Bowie, J. U., N. D. Clarke, C. O. Pabo, and R. T. Sauer. 1990. Identification of protein folds: matching hydrophobicity patterns of sequence sets with solvent accessibility patterns of known structures. *Proteins.* 7:257–264.

29. Ota, M., and K. Nishikawa. 1997. Assessment of pseudo-energy potentials by the best-five test: a new use of the three-dimensional profiles of proteins. *Protein Eng.* 10:339–351.

30. Sali, A., and T. L. Blundell. 1993. Comparative protein modelling by satisfaction of spatial restraints. *J. Mol. Biol.* 234:779–815.

31. Fiser, A., R. K. Do, and A. Sali. 2000. Modeling of loops in protein structures. *Protein Sci.* 9:1753–1773.

32. Baker, D., and A. Sali. 2001. Protein structure prediction and structural genomics. *Science.* 294:93–96.

33. Marti-Renom, M. A., M. S. Madhusudhan, A. Fiser, B. Rost, and A. Sali. 2002. Reliability of assessment of protein structure prediction methods. *Structure.* 10:435–440.

34. Achour, A., K. Persson, R. A. Harris, J. Sundback, C. L. Sentman, Y. Lindqvist, G. Schneider, and K. Karre. 1998. The crystal structure of H-2Dd MHC class I complexed with the HIV-1-derived peptide P18–I10 at 2.4 A resolution: implications for T cell and NK cell recognition. *Immunity.* 9:199–208.

35. Stewart, J. J. P. 1996. Application of localized molecular orbitales to the solution of semiempirical self-consistent field equations. *Int. J. Quant. Chem.* 58:133–146.

36. Sherman, D. H., P. S. Hochman, R. Dick, R. Tizard, K. L. Ramachandran, R. A. Flavell, and B. T. Huber. 1987. Molecular analysis of antigen recognition by insulin-specific T-cell hybridomas from B6 wild-type and bm12 mutant mice. *Mol. Cell. Biol.* 7:1865–1872.

37. Tan, K. N., B. M. Datlof, J. A. Gilmore, A. C. Kronman, J. H. Lee, A. M. Maxam, and A. Rao. 1988. The T cell receptor V alpha 3 gene segment is associated with reactivity to *p*-azobenzenearsonate. *Cell.* 54:247–261.

38. Bill, J., J. Yague, V. B. Appel, J. White, G. Horn, H. A. Erlich, and E. Palmer. 1989. Molecular genetic analysis of 178 I-Abm12-reactive T cells. *J. Exp. Med.* 169:115–133.

39. Cerasoli, D. M., M. P. Riley, F. F. Shih, and A. J. Caton. 1995. Genetic basis for T cell recognition of a major histocompatibility complex class II-restricted neo-self peptide. *J. Exp. Med.* 182:1327–1336.

40. Horwitz, M. S., Y. Yanagi, and M. B. Oldstone. 1994. T-cell receptors from virus-specific cytotoxic T lymphocytes recognizing a single immunodominant nine-amino-acid viral epitope show marked diversity. *J. Virol.* 68:352–357.

41. Plaksin, D., K. Polakova, P. McPhie, and D. H. Margulies. 1997. A three-domain T cell receptor is biologically active and specifically stains cell surface MHC/peptide complexes. *J. Immunol.* 158:2218–2227.

42. Bowie, J. U., R. Luthy, and D. Eisenberg. 1991. A method to identify protein sequences that fold into a known three-dimensional structure. *Science.* 253:164–170.

43. Kaye, J., and S. M. Hedrick. 1988. Analysis of specificity for antigen, Mls, and allogenic MHC by transfer of T-cell receptor alpha- and beta-chain genes. *Nature.* 336:580–583.

44. Lai, M. Z., Y. J. Jang, L. K. Chen, and M. L. Gefter. 1990. Restricted V-(D)-J junctional regions in the T cell response to lambda-repressor. Identification of residues critical for antigen recognition. *J. Immunol.* 144:4851–4856.

45. Bellio, M., Y. C. Lone, O. de la Calle-Martin, B. Malissen, J. P. Abastado, and P. Kourilsky. 1994. The V beta complementarity determining region 1 of a major histocompatibility complex (MHC) class I-restricted T cell receptor is involved in the recognition of peptide/MHC I and superantigen/MHC II complex. *J. Exp. Med.* 179: 1087–1097.

46. Lone, Y. C., M. Bellio, A. Prochnicka-Chalufour, D. M. Ojcius, N. Boissel, T. H. Ottenhoff, R. D. Klausner, J. P. Abastado, and P. Kourilsky. 1994. Role of the CDR1 region of the TCR beta chain in the binding to purified MHC-peptide complex. *Int. Immunol.* 6: 1561–1565.

47. Clark, S. P., B. Arden, D. Kabelitz, and T. W. Mak. 1995. Comparison of human and mouse T-cell receptor variable gene segment subfamilies. *Immunogenetics.* 42:531–540.

Available online at www.sciencedirect.com
ScienceDirect
ELSEVIER
Virology 367 (2007) 390–397
VIROLOGY
www.elsevier.com/locate/yviro

Chimeric adenovirus type 5/35 vector encoding SIV *gag* and HIV *env* genes affords protective immunity against the simian/human immunodeficiency virus in monkeys

Kenji Someya [a,b,c,*], Ke-Qin Xin [c], Yasushi Ami [d], Yasuyuki Izumi [b], Hiroyuki Mizuguchi [e], Shinrai Ohta [b,c], Naoki Yamamoto [b], Mitsuo Honda [b], Kenji Okuda [c]

[a] *Department of Virology III, National Institute of Infectious Diseases, Musashimurayama, Tokyo 208-0011, Japan*
[b] *AIDS Research Center, National Institute of Infectious Diseases, Shinjuku-ku, Tokyo 162-8640, Japan*
[c] *Department of Molecular Biodefense Research, Yokohama City University, School of Medicine, Kanazawa-ku Yokohama 236-0004, Japan*
[d] *Division of Experimental Animal Research, National Institute of Infectious Diseases, Musashimurayama, Tokyo 208-0011, Japan*
[e] *Laboratory of Gene Transfer and Regulation, National Institute of Biomedical Innovation, Ibaraki, Osaka 567-0085, Japan*

Received 29 March 2007; returned to author for revision 30 April 2007; accepted 14 June 2007
Available online 12 July 2007

Abstract

Replication-defective adenovirus type 5 (Ad5) vector-based vaccines are widely known to induce strong immunity against immunodeficiency viruses. To exploit this immunogenicity while overcoming the potential problem of preexisting immunity against human adenoviruses type 5, we developed a recombinant chimeric adenovirus type 5 with type 35 fiber vector (rAd5/35). We initially produced a simian immunodeficiency virus (SIV) *gag* DNA plasmid (rDNA-Gag), a human immunodeficiency virus type 1 (HIV-1) 89.6 *env* DNA plasmid (rDNA-Env) and a recombinant Ad5/35 vector encoding the SIV *gag* and HIV *env* gene (rAd5/35-Gag and rAd5/35-Env). Prime-boost vaccination with rDNA-Gag and -Env followed by high doses of rAd5/35-Gag and -Env elicited higher levels of cellular immune responses than did rDNAs or rAd5/35s alone. When challenged with a pathogenic simian human immunodeficiency virus (SHIV), animals receiving a prime-boost regimen or rAd5/35s alone maintained a higher number of $CD4^+$ T cells and remarkably suppressed plasma viral RNA loads. These findings suggest the clinical promise of an rAd5/35 vector-based vaccine.

Keywords: DNA vaccine; Recombinant Ad5/35; Cellular immunity; Pathogenic SHIV challenge

Introduction

HIV-specific cellular and humoral responses play a critical role in controlling viral replication and disease progression (Mascola, 2003; Letvin et al., 2002; Musey et al., 1997). It has been reported that recombinant live virus- and bacteria-based vaccines such as recombinant adenovirus (Mascola et al., 2005; Shiver et al., 2002) recombinant poxvirus (Someya et al., 2004; Amara et al., 2001), and recombinant BCG (Ami et al., 2005; Someya et al., 2005) elicited high levels of effective immunity against immunodeficiency viruses when used either alone or in conjunction with other vectors.

Adenoviruses, which are associated with benign pathologies in humans, are attractive for use in HIV vaccines because their genome has been extensively studied and because methods for constructing recombinant vectors with them are well established (Imler, 1995). A regimen that primes with DNA and then boosts with rAd5 is known to protect macaques against SHIV challenge by inducing high levels of viral-specific immunities (Shiver et al., 2002). However, Ad5 has been prevented from fully realizing its clinical potential (Catanzaro et al., 2006) because of preexisting humoral immunity to adenoviruses (Barouch et al., 2004; Casimiro et al., 2003). A previous study demonstrated that neutralizing antibodies against Ad5 are widespread in healthy blood donors in the developed world, whereas neutralizing

* Corresponding author. Department of Virology III, National Institute of Infectious Diseases 4-7-1 Gakuen, Musashimurayama, Tokyo 208-0011, Japan. Fax: +81 42 565 3315.
E-mail address: someyan@nih.go.jp (K. Someya).

0042-6822/$ - see front matter © 2007 Elsevier Inc. All rights reserved.
doi:10.1016/j.virol.2007.06.012

antibodies against Ad35 are rare (Kostense et al., 2004; Vogels et al., 2003). Furthermore, patients at risk of AIDS were reported to have a much higher seroprevalence of Ad5 than Ad35 (Kostense et al., 2004).

We have recently constructed an adenovirus serotype 5 vector that possesses serotype 35 fiber (rAd5/35) that encodes the simian immunodeficiency virus (SIV) *gag* gene or human immunodeficiency virus type 1 (HIV-1) IIIB *env* gp160 gene (Xin et al., 2005). The rAd5/35 vector, which lacks the E1 and E3 genes that are responsible for viral replication (Imler, 1995), interacts with CD46-expressing cells (Gaggar et al., 2003) and antigen-presenting cells (Rea et al., 2001). The rAd5/35 vector was shown to enter human dendritic cells (DC) more efficiently than Ad5 and activate T cells *ex vivo* (Ophorst et al., 2004), suggesting that a rAd5/35 vector-based vaccine may be an effective activator for T cell immunity. However, rAd5/35 vector-expressing measles virus hemagglutinin was less immunogenic than rAd5 in low-dose immunization in macaques and suggested that fiber exchange may not circumvent anti-Ad5 immunity during acute Ad5 infection in mice (Ophorst et al., 2004).

Recently, hyper variable regions on the Ad5 hexon protein were successfully replaced with those of the rare Ad48, allowing preexisting anti-vector immunity to be circumvented (Roberts et al., 2006). We previously showed that, when combined with plasmid DNA, the rAd5/35 vector elicited high levels of cellular responses that in turn protected mice from challenge with a virulent vaccinia virus encoding HIV-1 BH8 env (Xin et al., 2005). Furthermore, the rAd5/35 vector-based vaccine was not affected by the preexisting anti-Ad5 immunity in mice.

These results suggest that a vaccine combining plasmid DNA and the rAd5/35 vector may induce effective viral-specific immunities in macaques. In this study, we determined the vaccine efficacy of relatively high doses of rAd5/35 vector-based HIV vaccine in an SHIV macaque model.

Results

Vaccine-induced T cell responses to SIV Gag and HIV Env

After priming with rDNA-Gag and rDNA-Env, Gag- and Env-specific IFN-γ spot-forming cells (SFC) were detected in both the rDNA and the prime-boost groups (Fig. 1A). The numbers of SFC against Gag peaked at 16 weeks in the rDNA and the prime-boost groups, with numbers averaging 120 in the rDNA group and 128 in the prime-boost group. ELISPOT responses to Env also peaked at 16 weeks, with average numbers of 33 in the rDNA group and of 66 in the prime-boost group. Gag- and Env-specific ELISPOT responses were not observed in animals immunized with cDNA (SFC ≤ 10).

Two serial high-dose injections with rAd5/35-Gag and rAd5/35-Env per animal dramatically augmented Gag- and Env-specific ELISPOT responses in the prime-boost group (Fig. 1A). At Week 150, the prime-boost group averaged 53 Gag-specific and 35 Env-specific SFC. Two weeks after the two serial injections with rAd5/35 (154 weeks), the average number of Gag-specific SFC increased to 1073 and that of Env-specific SFC to 340. Two serial injections with rAd5/35s also elicited higher ELISPOT responses in the rAd5/35 group (Fig. 1A), with the average number of Gag-specific SFC increasing from 35 to 570 and that of Env-specific SFC, from 15 to 165. The levels of both Gag and Env ELISPOT responses at the time of virus challenge (154 weeks) significantly increased in the prime-boost group, and they were higher than those in the rDNA (Gag, $p<0.01$; ENV, $p<0.01$) and the cDNA (Gag, $p<0.01$; Env, $p<0.01$) groups. Serial injections with cAd5/35s failed to enhance responses to Gag or Env in either the rDNA or the cDNA group.

Vaccine-induced antibody responses to SIV Gag and HIV Env

Both anti-Gag- and Env-specific IgG responses were detected after serial inoculations with rDNA-Gag and rDNA-Env (Fig. 1B). Anti-Gag-specific IgG titers peaked at 16 weeks in the rDNA group, averaging 123 and at 32 weeks in the prime-boost group, averaging 155 (Fig. 1B, upper panel). The anti-Env-specific IgG titers for both the rDNA and the prime-boost groups peaked at 32 weeks, with titers of 200 and 183, respectively (Fig. 1B, lower panel). Two serial injections with rAd5/35-Gag and rAd5/35-Env to the prime-boost group enhanced both anti-Gag- and anti-Env-specific IgG titers, with the former increasing from an average of 100 at 150 weeks to an average of 823 at 154 weeks and the latter increasing from an average of 74 at 150 weeks to 2240 at 154 weeks. Two serial injections with rAd5/35-Gag and rAd5/35-Env to the rAd5/35 group generated both anti-Gag- and anti-Env-specific IgG responses, with the peak titers in the former averaging 335 and in the latter, 480. Both the anti-Gag- and Env-specific IgG titers at the time of virus challenge (154 weeks) in the prime-boost group were significantly higher than those in the rDNA (Gag, $p<0.01$; Env, $p<0.01$) and the cDNA (Gag, $p<0.01$; Env, $p<0.01$) groups. When anti-HIV-89.6-specific neutralization antibody responses were measured at 154 weeks using the purified serum IgG, the rDNA, the rAd35 and the prime-boost groups showed an average neutralization of 4%, 10% and 24% respectively (data not shown), suggesting that the antibody may not contribute to the partial protection from virus challenge in monkeys. Two serial injections with Ad5/35-LacZ had no effect on anti-Gag and anti-Env IgG responses.

Plasma viral RNA loads and $CD4^+$ T cell counts after challenge with SHIV

To evaluate the efficacy of a prime-boost vaccine regimen, all animals received an intravenous challenge with 20 $TCID_{50}$ of highly pathogenic SHIV at 154 weeks (Table 1). Peak plasma RNA loads (Fig. 2A) and rapid or transient $CD4^+$ T cell loss (Fig. 2B) were observed within 2 weeks after challenge (acute phase). The cDNA group had the greatest viral RNA loads (peaking at an average of 4.5×10^9 copies/ml) and experienced dramatic loss of $CD4^+$ T cells (≤ 50 cells/μl). Although its peak viral RNA loads (an average of 4.9×10^8 copies/ml) were almost ten-fold less than those of the cDNA group ($p<0.01$), the rDNA group likewise showed reduced $CD4^+$ T cell numbers

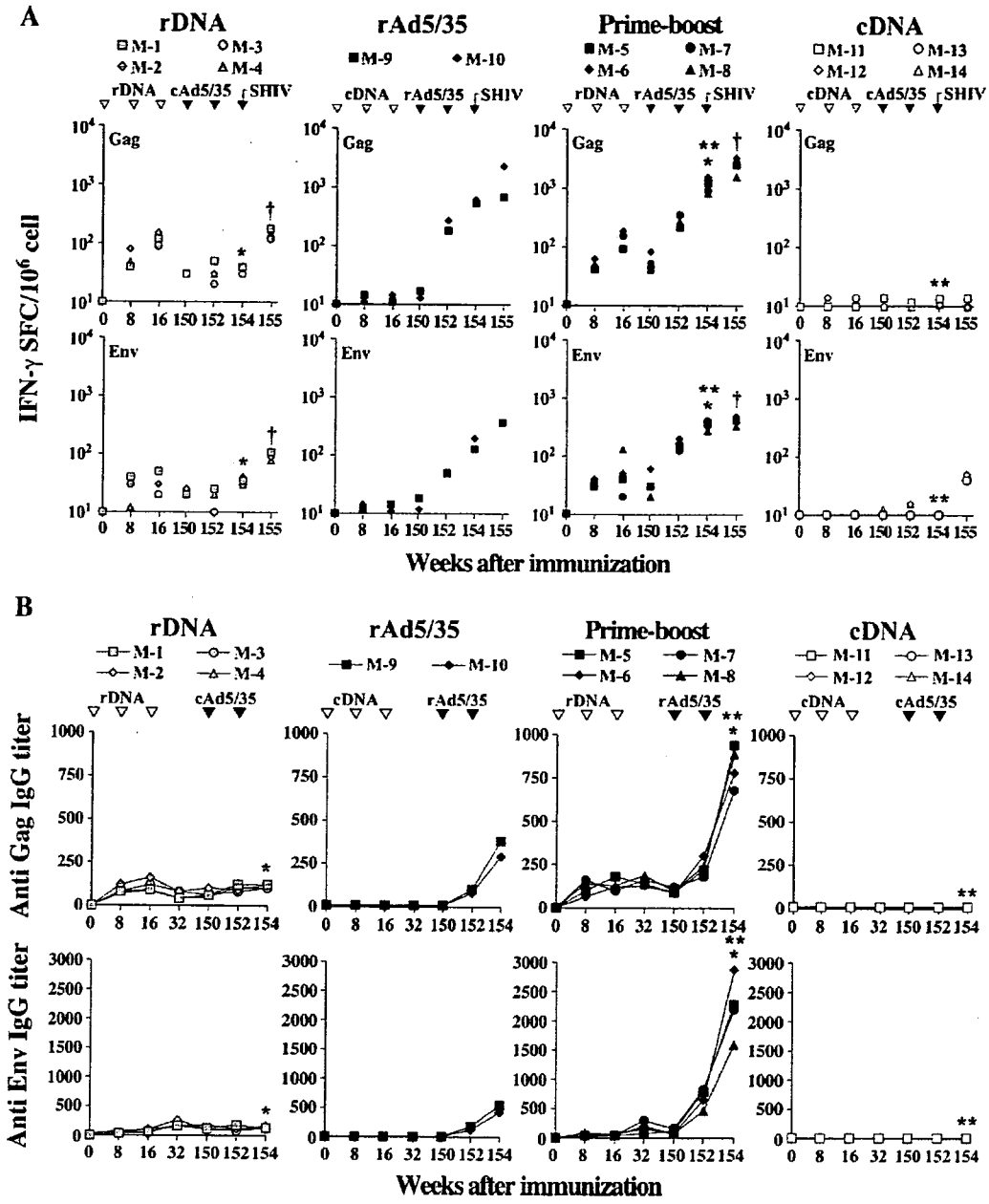

Fig. 1. Cellular and humoral responses of vaccinated animals. (A) Freshly isolated PBMC were stimulated with SIV Gag and HIV Env peptides. An ELISPOT assay was used to monitor the numbers of antigen-specific IFN-γ spot-forming cells. *rDNA vs. prime-boost, $p<0.01$ (154 weeks). **Prime-boost vs. cDNA, $p<0.01$ (154 weeks). †rDNA vs. prime-boost group, $p<0.01$ (155 weeks). (B) End-point Gag- and Env-specific plasma IgG titers were determined in the course of immunization using ELISA. *rDNA vs. prime-boost, $p<0.01$ (154 weeks). **Prime-boost vs. cDNA, $p<0.01$ (154 weeks).

(≤ 40 cells/μl, no significance). The prime-boost group showed greater than 600-fold reduction in peak viral loads and maintained higher $CD4^+$ T cell numbers compared to the cDNA group (the peak viral loads of the prime-boost group in the acute viral phase: an average of 7.3×10^6 copies/ml, $p<0.01$; $CD4^+$ T cell numbers of the prime-boost group: an average of 616 cells/μl, $p<0.01$). The initial viremia and $CD4^+$ T cell numbers in the prime-boost group were also significantly lower than those in the rDNA group (peak viral RNA loads, $p<0.01$; $CD4^+$ T cell numbers, $p<0.01$). The rAd5/35 group showed 600-fold reduction in the peak viral loads (an average of 5.3×10^6 copies/ml) compared to the cDNA group and maintained higher $CD4^+$ T cell numbers (an average of 500 cells/μl).

During the set-point phase, the cDNA group showed higher viral RNA loads ($\geq 5\times10^6$ copies/ml) and lower $CD4^+$ T cell numbers (≤ 20 cells/μl) (Fig. 2). The set-point viral RNA loads of the rDNA group (averaging 10^6 copies/ml) were approximately five-fold lower than those of the control group, but the $CD4^+$ T cell numbers recovered by no more than 100 cells/μl. Two animals (M-5 and M-6) of the prime-boost group showed well-controlled set-point viral loads and minimal $CD4^+$ T cells

Table 1
Immunization and challenge schedule

Group (regimen)	Monkey no.	Priming immunization and route	Schedule (week of priming)	Booster immunization and route	Schedule (week of boosting)	SHIV challenge
rDNA	M-1, M-2, M-3, M-4	rDNA-Gag, 2.5 mg, i.m. and rDNA-Env, 2.5 mg, i.m.	0, 8, 16	cAd5/35, 2×10^{11} vp, i.d.	150, 152	20 $TCID_{50}$, i.v., Week 154
Prime-boost	M-5, M-6, M-7, M-8	rDNA-Gag, 2.5 mg, i.m. and rDNA-Env, 2.5 mg, i.m.	0, 8, 16	rAD3/35-Gag, 10^{11} vp, i.d. and rAD3/35-Env, 10^{11} vp, i.d.	150, 152	20 $TCID_{50}$, i.v., Week 154
rAd5/35	M-9, M-10	cDNA, 5 mg, i.m.	0. 8, 16	rAD3/35-Gag, 10^{11} vp, i.d. and rAD3/35-Env, 10^{11} vp, i.d.	150, 152	20 $TCID_{50}$, i.v., Week 154
cDNA	M-11, M-12, M-13, M-14	cDNA, 5 mg, i.m.	0. 8, 16	cAd5/35, 2×10^{11} vp, i.d.	150, 152	20 $TCID_{50}$, i.v., Week 154

loss, while the other two macaques (M-7 and M-8) of the same group showed slightly higher viral RNA loads and lower $CD4^+$ T cell numbers. The set-point viral RNA loads for M-6 were within the detection limit (500 copies/ml) and those for M-5 ranged from <500 to 3×10^3 copies/ml. The viremia-controlled M-6 showed more than 800 $CD4^+$ T cells/μl and M-5 showed 600 cells/μl, with the exception of the transient loss (about 350 cells/μl) occurring at 6 and 18 weeks. Set-point viral RNA loads for both M-7 and M-8 ranged from 3.7×10^3 to 4.2×10^4 copies/ml, while $CD4^+$ T cell numbers ranged from 300 to 600 cells/μl. Of the two macaques in the rAd5/35 group, one showed enhanced protection, while the other did not. M-9 suppressed viral loads to less than 10^4 copies/ml and maintained $CD4^+$ T cell numbers at levels of more than 500 cells/μl. The viral loads for M-10 ranged from 10^5 to 10^6 copies/ml, and its $CD4^+$ T cell numbers were less than 300 cells/μl. Throughout the set-point phase, average plasma viral RNA loads and $CD4^+$ T cell numbers in the prime-boost group were significantly different compared to those in the cDNA (plasma viral RNA loads, $p<0.01$; $CD4^+$ T cell numbers, $p<0.01$) and rDNA (plasma viral RNA loads, $p<0.01$; $CD4^+$ T cell numbers, $p<0.01$) groups.

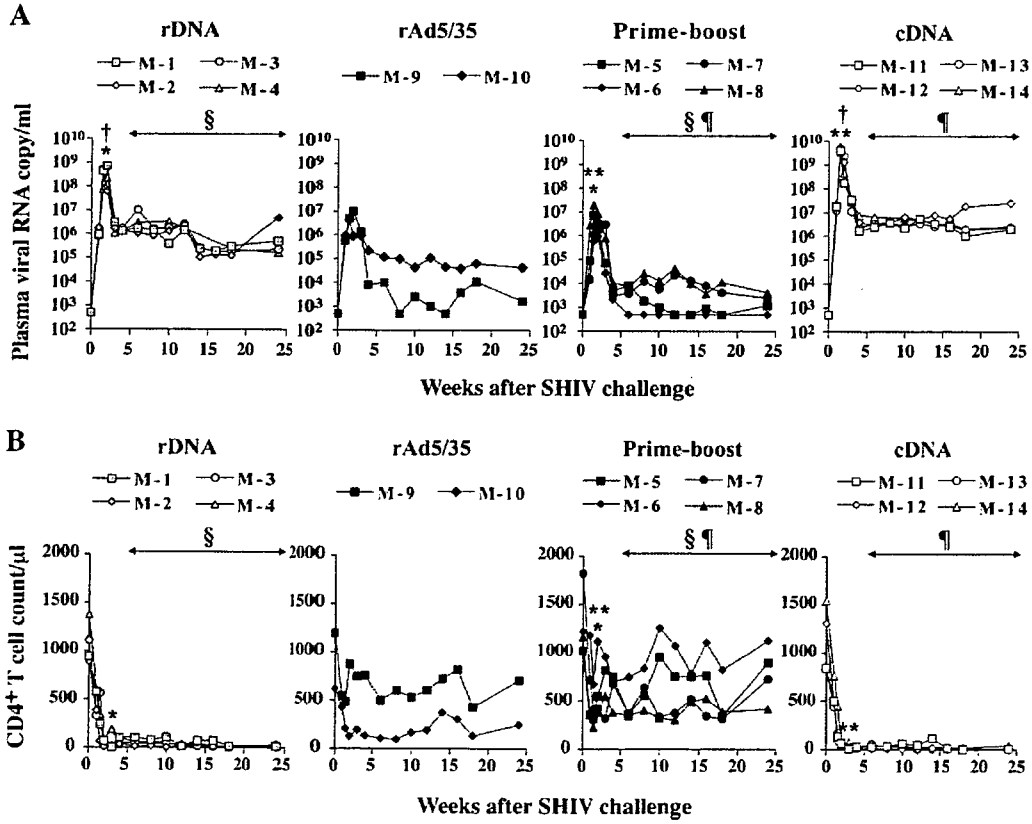

Fig. 2. Plasma viral RNA loads and $CD4^+$ T cell counts after challenge with SHIV. (A) Plasma RNA copies were determined by quantitative RT-PCR with a detection limit of 500 viral RNA copies per ml. *rDNA vs. prime-boost, $p<0.01$ (acute phase). **Prime-boost vs. cDNA, $p<0.01$ (acute phase). †rDNA vs. cDNA, $p<0.01$ (acute phase). §rDNA vs. prime-boost, $p<0.01$ (set-point phase). ¶Prime-boost vs. cDNA, $p<0.01$ (set-point phase). (B) Whole blood was stained with CD3 and CD4 antibodies. $CD4^+$ T cell numbers were determined using flow cytometry. *rDNA vs. prime-boost, $p<0.01$ (acute phase). **Prime-boost vs. cDNA, $p<0.01$ (acute phase). §rDNA vs. prime-boost, $p<0.01$ (set-point phase). ¶Prime-boost vs. cDNA, $p<0.01$ (set-point phase).

T cells immune response to Gag and Env after challenge with SHIV

At an early phase of infection (1 week after challenge), IFN-γ ELISPOT responses showed that the prime-boost group had higher numbers of Gag- and Env-specific SFC (Gag specific, an average of 2385; Env specific, an average of 420) than those of the rAd5/35 group (Gag specific, an average of 920; Env specific, an average of 270) (Fig. 2A). Furthermore, lower numbers of SFC were seen in the rDNA group (an average of 153 SFC specific for Gag; an average of 103 SFC specific for Env) than those in the prime-boost group (Gag, $p<0.01$; Env, $p<0.01$). The cDNA group showed no responses (≤ 30 SFC). Taken together, these results suggest that the prime-boost regimen elicited the highest frequency of cellular memory T cells in response to viral challenge.

Discussion

Higher plasma viral RNA loads and lower $CD4^+$ T cell numbers have been linked to disease progression in HIV-infected individuals (Patke et al., 2002; Mellors et al., 1996, 1997), suggesting that the generation of robust HIV-specific immunity may be critical in the control of viral infection. Recently, it was shown that a recombinant Ad5 vector-based HIV vaccine induced high levels of cellular immunity and protected animals from highly pathogenic viral challenge (Shiver et al., 2002). In contrast, other studies have shown that preexisting anti-Ad5 immunity can attenuate the efficacy of recombinant Ad5-based HIV vaccine (Barouch et al., 2004; Kostense et al., 2004; Casimiro et al., 2003). It is essential that such preexisting anti-Ad5 immunity be overcome if we are to enjoy the benefits offered by Ad5 as a vaccine vector, such as its induction of strong T cell immunity. Rare serotype Ad35, which is classified into subgroup B, has different cell tropism from Ad5 (Marttila et al., 2005; Segerman et al., 2000; Shayakhmetov et al., 2000; De Jong et al., 1997), and the seroprevalence of Ad35 in immunocompromised individuals and those at risk of AIDS was lower than that of Ad5, suggesting that Ad35 could be used as the base for an HIV vaccine (Kostense et al., 2004; Vogels et al., 2003). Therefore, the advantage of constructing a chimeric Ad5/35 vaccine is that the vector will retain its infectivity with less risk of preexisting immunity against the vaccine vector than that of Ad5-based vaccine. This suggests that the Ad5/35 vaccine would allow the basis for adenoviral vectors to be broadened with improved properties.

In this study, we initially constructed Ad5/35 vector-based HIV vaccine and demonstrated that its immunogenicity and protective efficacy in a macaque model. The rAd5/35 vector was previously developed as a vaccine vehicle for DC targeting (Xin et al., 2005, 2007; Mizuguchi and Hayakawa, 2002), and the rAd5/35 vector showed much lower hepatotoxicity than Ad5 (Xin et al., 2005). Recently, Ophorst et al. (2004) reported that rAd5 vector carrying a part of the fiber molecule of Ad35 (rAd5. Fib35) was less immunogenic in monkeys than rAd5, and rAd5. Fib35 showed no significant difference in anti-insert immunity over Ad5 in mice with high Ad5 vector-specific immunity. In addition, Abbink et al. (2007) reported comparative seroprevalence and immunogenicity studies involving rAd11, rAd35 and rAd50 vectors from subgroup B, rAd26, rAd48 and rAd49 vectors from subgroup D and rAd5 vectors from subgroup C. These rAd vectors were rare serotypes and elicited Gag-specific cellular immune responses in mice both with and without anti-Ad5 immunity. However, the rare serotype-based rAd vectors have proven less immunogenic than rAd5 vectors in animal models in spite of the absence of anti-Ad5 immunity (Barouch et al., 2004; Lemckert et al., 2005). In our previous study, rAd5/35 vector was highly immunogenic and significantly less susceptible to preexisting anti-Ad5 immunity than a comparable Ad5 vector (Xin et al., 2005). Although we did not compare the rAd5/35 vector directly with other serotype rAd vectors, we demonstrated that the rAd5/35 vector was immunogenic, and a much higher degree of immunogenicity was achieved by adopting a prime-boost regimen combining rAd5/35 vectors with rDNA vaccine in macaques.

To evaluate the efficacy of the vaccine, we monitored T cell responses, plasma viral RNA loads and $CD4^+$ T cell numbers following SHIV challenge. In the present study, we used highly pathogenic SHIV-C2/1 (Shinohara et al., 1998), which originated from SHIV 89.6 (Lu et al., 1996; Reimann et al., 1996) because our vaccine regimen was designed to target SIV Gag and HIV Env antigens and for the virus to well reproduce high plasma viremia and loss of $CD4^+$ cells (Eda et al., 2006; Someya et al., 2005, 2006; Ami et al., 2005; Shinohara et al., 1998).

After challenge with SHIV, all animals in the prime-boost and the rAd5/35 groups showed high memory T cell responses against Gag and Env, and these animals showed a reduction in peak viral RNA loads at the acute phase of infection. Furthermore, in the set-point phase, two animals in the prime-boost group and one animal in the rAd5/35 group controlled SHIV infection, and the remaining two animals in the prime-boost and one animal in the rAd5/35 groups showed moderate control. In spite of higher cellular responses being observed in the prime-boost group than those in the rAd5/35 group, the difference in protective levels between the prime-boost and the rAd5/35 groups was not clearly separated. Although it is not possible to directly compare the levels of immune responses and protective efficacy induced by the rAd5/35 vector to those of other rAd vector studies, our results appeared to be similar to those obtained with the other rAds (Abbink et al., 2007; Barratt-Boyes et al., 2006; Ophorst et al., 2004; Shiver et al., 2002; Musey et al., 1997). To clarify the efficacy of the rAd5/35 vector, further studies to compare with other rAd vectors may be needed. However, our results suggest that the rAd5/35 vector-based vaccine either alone or combined with DNA vaccine elicited a high frequency of viral-specific cellular T cell response that may well be key to controlling the acute and chronic phases of infection.

In conclusion, we have demonstrated that high doses of rAd5/35 vector-based vaccine afford protective immunity against SHIV in macaques. Since the rAd5/35 vector-based vaccine can bypass preexisting anti-Ad5 immunity, therAd5/35-based vaccine may offer considerable promise as an HIV vaccine.

Materials and methods

Animals

Fourteen adult cynomolgus macaques (*Macaca fascicularis*) were used in this study. The macaques were fed and cared for in accordance with the standard operating procedure approved by the Ministry of Education, Culture, Sports, Science and Technology of Japan. The study was performed in the P3 facility under guidelines established by the laboratory biosafety manual of World Health Organization (Someya et al., 2005).

Preparation of DNA and recombinant adenoviral vectors

A eukaryotic expression plasmid, pcDNA3.1 (−) (Invitrogen, Carlsbad, CA), was used as a backbone of the DNA vaccines that encode the SIVmac239 *gag* gene (rDNA-Gag) and HIV-1 89.6 *env* gp160 gene (rDNA-Env), and both DNA vaccines were constructed as previously described according to the standard protocol (Someya et al., 2004). The SIV and HIV DNAs for the DNA vaccines were not modified using humanized codon. No foreign gene encoding pcDNA 3.1 (−) was used as a control DNA vaccine (cDNA).

The E1 and E3 regions deleted recombinant Ad5/35 vectors that encoded the SIVmac239 *gag* gene (rAd5/35-Gag) and HIV-1 89.6 *env* gp160 gene (rAd5/35-Env) were constructed with an Ad generation kit (Avior Therapeutics, Inc., Seattle, WA) as previously described (Xin et al., 2005; Mizuguchi and Hayakawa, 2002). Briefly, SIV *gag* and HIV *env* PCR fragments driven by a CAG promoter were inserted into a shuttle plasmid, pLHSP (Avior Therapeutics, Inc.), before being transfected to human embryonic kidney (HEK293) cells. The recombinant vectors were purified by CsCl gradient centrifugation, and the total concentration of virus particles was calculated from the optical density at 260 nm (OD_{260}), using the formula 1 $OD_{260} = 1 \times 10^{12}$ virus particles/ml.

Immunizations and viral challenge

Four animals of the rDNA group (numbered M-1 through M-4) received three intramuscular injections of both 2.5 mg of rDNA-Gag and 2.5 mg of rDNA-Env at 8-week intervals (Weeks 0, 8 and 16), followed by two intradermal injections of control Ad5/35 expressing the gene LacZ (cAd5/35, 2×10^{11} particles of each) at 2-week intervals (Weeks 150 and 152). Four animals of the prime-boost group (numbered M-5 through M-8) received three injections of both 2.5 mg of rDNA-Gag and 2.5 mg of rDNA-Env, followed by two injections with both 10^{11} particles of rAd5/35-Gag and 10^{11} particles of rAd5/35-Env. Two animals of the rAd5/35 group (numbered M-9 and M-10) received three injections of 5 mg of cDNA, followed by two injections with both 10^{11} particles of rAd5/35-Gag and 10^{11} particles of rAd5/35-Env. The four control animals of the control group (numbered M-11 through M-14) received three injections of 5 mg of cDNA, followed by two injections with 2×10^{11} particles of cAd5/35 (Table 1). All animals received an intravenous challenge with twenty 50% tissue culture infectious doses ($TCID_{50}$) of highly pathogenic SHIV that originated from SHIV-89.6 (Someya et al., 2006; Shinohara et al., 1998, Lu et al., 1996; Reimann et al., 1996) 2 weeks after final immunization (at 154 weeks, Table 1).

Cellular immune response to SIV Gag and HIV Env

The cellular immune responses against SIV Gag and HIV Env were monitored by IFN-γ ELISPOT assay using SIVmac239 Gag peptide pools spanning the full length of the Gag protein and HIV-89.6 Env V3 peptides as previously described (Someya et al., 2005, 2006). Freshly isolated peripheral blood mononuclear cells were added to 96-well plates in triplicate at 2×10^5 cells/well and then incubated for 16 h with Gag peptide pools or V3 peptide. Individual IFN-γ spot-forming cells (SFC) were counted by using a KS ELISPOT compact system (Carl Zeiss, Jena, Germany). An SFC was defined as a large black spot with a fuzzy border (Mothe et al., 2002).

Antibody responses to SIV Gag and HIV Env

The humoral immune responses were determined by measuring anti-Gag- and anti-Env-specific IgG titers using ELISA as previously described (Someya et al., 2005, 2006). Ninety-six-well ELISA plates were coated with 1 μg/ml of SIV p27 Gag (Advanced Biotechnologies, Advanced Biotechnologies, Woburn, MA) or 5 μg/ml of SHIV 89.6P Env peptide (AIDS Research and Reference Program, National Institutes of Health, Rockville, MD). Heat-inactivated sera were serially diluted and then added to the ELISA plate. Anti-Gag- and-Env-V3-specific IgG bound to the antigens were detected with alkaline phosphatase-labeled goat anti-monkey IgG (EY Laboratories, Inc., San Mateo, CA) and *p*-nitrophenyl-phosphate disodium substrate (Invitrogen, Carlsbad, CA).

The SHIV-specific neutralization antibody assay was performed as previously described (Someya et al., 2005, 2006). In brief, 5 μg/ml of purified serum IgG was incubated with 100 $TCID_{50}$ of SHIV-C2/1 and then cultured in M8166 cells. The result was compared with cultures to which preimmune IgG had been added. Neutralization was expressed as the percent inhibition of SIV Gag production in the culture supernatant. The average results + 6 SD of serum Ig from normal healthy monkeys were used as the cutoff for a positive titer (Someya et al., 2006).

Plasma viral RNA levels and $CD4^+$ T cell counts

SHIV RNA levels in plasma samples were determined by real-time PCR with a PRISM 7700 sequence detection system (Perkin-Elmer Applied Biosystems, Forest City, CA) as previously described (Someya et al., 2006; Sasaki et al., 2002). All RNA samples were amplified in duplicate. Data were expressed as RNA copies per milliliter.

$CD4^+$ T cell numbers were measured using a FACS Calibur flow cytometer system (Becton-Dickinson Bioscience, San Jose, CA) as previously described (Someya et al., 2006; Yoshino et al., 2000). Fifty microliters of whole blood specimens was stained

with anti-human CD3 (clone HIT3a, Becton-Dickinson), anti-human CD4 (clone SK3 Becton-Dickinson) and anti-human CD8 (clone SK1, Becton-Dickinson). CD3/CD4 effective T cell counts were analyzed using Cell Quest software (Becton-Dickinson).

Statistical analysis

Comparisons of test results among groups of animals were performed using the Kruskal–Wallis *H*-test followed by Student–Newman–Keuls correction.

Acknowledgments

We thank Dr. Nao Jounai of the Department of Molecular Biodefense Research, Yokohama City University, School of Medicine for his technical support.

References

Abbink, P., Lemckert, A.A., Ewald, B.A., Lynch, D.M., Denholtz, M., Smits, S., Holterman, L., Damen, I., Vogels, R., Thorner, A.R., O'Brien, K.L., Carville, A., Mansfield, K.G., Goudsmit, J., Havenga, M.J., Barouch, D.H., 2007. Comparative seroprevalence and immunogenicity of six rare serotype recombinant adenovirus vaccine vectors from subgroups B and D. J. Virol. 81, 4654–4663.

Amara, R.R., Villinger, F., Altman, J.D., Lydy, S.L., O'Neil, S.P., Staprans, S.I., Montefiori, D.C., Xu, Y., Herndon, J.G., Wyatt, L.S., Candido, M.A., Kozyr, N.L., Earl, P.L., Smith, J.M., Ma, H.L., Grimm, B.D., Hulsey, M.L., McClure, H.M., McNicholl, J.M., Moss, B., Robinson, H.L., 2001. Control of a mucosal challenge and prevention of AIDS by a multiprotein DNA/MVA vaccine. Science 292, 69–74.

Ami, Y., Izumi, Y., Matsuo, K., Someya, K., Kanekiyo, M., Horibata, S., Yoshino, N., Sakai, K., Shinohara, K., Yamazaki, S., Yamamoto, N., Honda, M., 2005. Prime-boost vaccination with recombinant Mycobacterium bovis Bacillus Calmette Guérin and a non-replicating vaccinia virus recombinant leads to long-lasting and effective immunity. J. Virol. 79, 12871–12879.

Barouch, D.H., Pau, M.G., Custers, J.H., Koudstaal, W., Kostense, S., Havenga, M.J., Truitt, D.M., Sumida, S.M., Kishko, M.G., Arthur, J.C., Korioth-Schmitz, B., Newberg, M.H., Gorgone, D.A., Lifton, M.A., Panicali, D.L., Nabel, G.J., Letvin, N.L., Goudsmit, J., 2004. Immunogenicity of recombinant adenovirus serotype 35 vaccine in the presence of pre-existing anti-Ad5 immunity. J. Immunol. 15, 6290–6297.

Barratt-Boyes, S.M., Soloff, A.C., Gao, W., Nwanegbo, E., Liu, X., Rajakumar, P.A., Brown, K.N., Robbins, P.D., Murphey-Corb, M., Day, R.D., Gambotto, A., 2006. Broad cellular immunity with robust memory responses to simian immunodeficiency virus following serial vaccination with adenovirus 5- and 35-based vectors. J. Gen. Virol. 87 (Pt. 1), 139–149.

Casimiro, D.R., Chen, L., Fu, T.M., Evans, R.K., Caulfield, M.J., Davies, M.E., Tang, A., Chen, M., Huang, L., Harris, V., Freed, D.C., Wilson, K.A., Dubey, S., Zhu, D.M., Nawrocki, D., Mach, H., Troutman, R., Isopi, L., Williams, D., Hurni, W., Xu, Z., Smith, J.G., Wang, S., Liu, X., Guan, L., Long, R., Trigona, W., Heidecker, G.J., Perry, H.C., Persaud, N., Toner, T.J., Su, Q., Liang, X., Youil, R., Chastain, M., Bett, A.J., Volkin, D.B., Emini, E.A., Shiver, J.W., 2003. Comparative immunogenicity in rhesus monkeys of DNA plasmid, recombinant vaccinia virus, and replication-defective adenovirus vectors expressing a human immunodeficiency virus type 1 *gag* gene. J. Virol. 77, 6305–6313.

Catanzaro, A.T., Koup, R.A., Roederer, M., Bailer, R.T., Enama, M.E., Moodie, Z., Gu, L., Martin, J.E., Novik, L., Chakrabarti, B.K., Butman, B.T., Gall, J.G.D., Richter King, C., Andrews, C.A., Sheets, R., Gomez, P.L., Mascola, J.R., Nabel, G.J., Graham, B.S., the Vaccine Research Center 006 Study Team, 2006. Phase 1 safety and immunogenicity evaluation of a multiclade HIV-1 candidate vaccine delivered by a replication-defective recombinant adenovirus vector. J. Infect. Dis. 194, 1638–1649.

De Jong, J.C., Wermenbol, A.G., Verweij-Uijterwaal, M.W., Slaterus, K.W., Wertheim-Van Dillen, P., Van Doornum, G.J., Khoo, S.H., Hierholzer, J.C., 1997. Adenoviruses from human immunodeficiency virus-infected individuals, including two strains that represent new candidate serotypes Ad50 and Ad51 of species B1 and D, respectively. J. Clin. Microbiol. 37, 3940–3945.

Eda, Y., Murakami, T., Ami, Y., Nakasone, T., Takizawa, M., Someya, K., Kaizu, M., Izumi, Y., Yoshino, N., Matsushita, S., Higuchi, H., Matsui, H., Shinohara, K., Takeuchi, H., Koyanagi, Y., Yamamoto, N., Honda, M., 2006. Anti-V3 humanized antibody KD-247 effectively suppresses ex vivo generation of human immunodeficiency virus type 1 and affords sterile protection of monkeys against a heterologous simian/human immunodeficiency virus infection. J. Virol. 80, 5563–5570.

Gaggar, A., Shayakhmetov, D.M., Lieber, A., 2003. CD46 is a cellular receptor for group B adenoviruses. Nat. Med. 9, 1408–1412.

Imler, J.L., 1995. Adenovirus vectors as recombinant viral vaccines. Vaccine 13, 1143–1151.

Kostense, S., Koudstaal, W., Sprangers, M., Weverling, G.J., Penders, G., Helmus, N., Vogels, R., Bakker, M., Berkhout, B., Havenga, M., Goudsmit, J., 2004. Adenovirus types 5 and 35 seroprevalence in AIDS risk groups supports type 35 as a vaccine vector. AIDS 18, 1213–1216.

Lemckert, A.A., Sumida, S.M., Holterman, L., Vogels, R., Truitt, D.M., Lynch, D.M., Nanda, A., Ewald, B.A., Gorgone, D.A., Lifton, M.A., Goudsmit, J., Havenga, M.J., Barouch, D.H., 2005. Immunogenicity of heterologous prime-boost regimens involving recombinant adenovirus serotype 11 (Ad11) and Ad35 vaccine vectors in the presence of anti-ad5 immunity. J Virol. 79, 9694–9701.

Letvin, N.L., Barouch, D.H., Montefiori, D.C., 2002. Prospect for vaccine protection against HIV-1 Infection and AIDS. Annu. Rev. Immunol. 20, 73–99.

Lu, Y., Salvato, M.S., Pauza, C.D., Li, J., Sodroski, J., Manson, K., Wyand, M., Letvin, N., Jenkins, S., Touzjian, N., Chutkowski, C., Kushner, N., LeFaile, M., Payne, L.G., Roberts, B., 1996. Utility of SHIV for testing HIV-1 vaccine candidates in macaques. J. Acquired Immune Defic. Syndr. Hum. Retrovirol. 12, 99–106.

Marttila, M., Persson, D., Gustafsson, D., Kathryn Liszewski, M.K., John, P., Atkinson, J.P., Wadell, G., Niklas Arnberg, N., 2005. CD46 is a cellular receptor for all species B adenoviruses except types 3 and 7. J. Virol. 79, 14429–14436.

Mascola, J.R., 2003. Defining the protective antibody response for HIV-1. Curr. Mol. Med. 3, 209–216.

Mascola, J.R., Sambor, A., Beaudry, K., Santra, S., Welcher, B., Louder, M.K., Vancott, T.C., Huang, Y., Chakrabarti, B.K., Kong, W.P., Yang, Z.Y., Xu, L., Montefiori, D.C., Nabel, G.J., Letvin, N.L., 2005. Neutralizing antibodies elicited by immunization of monkeys with DNA plasmids and recombinant adenoviral vectors expressing human immunodeficiency virus type 1 proteins. J. Virol. 79, 771–779.

Mellors, J.W., Rinaldo, C.R.Jr., Gupta, P., White, R.M., Todd, J.A., Kingsley, L.A., 1996. Prognosis in HIV-1 infection predicted by the quantity of virus in plasma. Science 272, 1167–1170.

Mellors, J.W., Munoz, A., Giorgi, J.V., Margolick, J.B., Tassoni, C.J., Gupta, P., Kingsley, L.A., Todd, J.A., Saah, A.J., Detels, R., Phair, J.P., Rinaldo Jr., C.R., 1997. Plasma viral load and $CD4^+$ lymphocytes as prognostic markers of HIV-1 infection. Ann. Intern. Med. 126, 946–954.

Mizuguchi, H., Hayakawa, T., 2002. Adenovirus vectors containing chimeric type 5 and type 35 fiber proteins exhibit altered and expanded tropism and increase the size limit of foreign genes. Gene 285, 69–77.

Mothe, B.R., Horton, H., Carter, D.K., Allen, T.M., Liebl, M.E., Skinner, P., Vogel, T.U., Fuenger, S., Vielhuber, K., Rehrauer, W., Wilson, N., Franchini, G., Altman, J.D., Haase, A., Picker, L.J., Allison, D.B., Watkins, D.I., 2002. Dominance of CD8 responses specific for epitopes bound by a single major histocompatibility complex class I molecule during the acute phase of viral infection. J. Virol. 76, 875–884.

Musey, L., Hughes, J., Schacker, T., Shea, T., Corey, L., McElrath, M.L., 1997. Cytotoxic T-cell responses, viral load, and disease progression in early human immunodeficiency virus type 1 infection. N. Engl. J. Med. 30, 1267–1274.

Ophorst, O.J., Kostense, S., Goudsmit, J., De Swart, R.L., Verhaagh, S., Zakhartchouk, A., Van Meijer, M., Sprangers, M., Van Amerongen, G., Yuksel, S., Osterhaus, A.D., Havenga, M.J., 2004. An adenoviral type 5 vector carrying a type 35 fiber as a vaccine vehicle: DC targeting, cross neutralization, and immunogenicity. Vaccine 22, 3035–3044.

Patke, D.S., Langan, S.J., Carruth, L.M., Keating, S.M., Sabundayo, B.P., Margolick, J.B., Quinn, T.C., Bollinger, R.C., 2002. Association of Gag-specific T lymphocyte responses during the early phase of human immunodeficiency virus type 1 infection and lower virus load set point. J. Infect. Dis. 186, 1177–1180.

Rea, D., Havenga, M.J., van Den Assem, M., Sutmuller, R.P., Lemckert, A., Hoeben, R.C., Bout, A., Melief, C.J., Offringa, R., 2001. Highly efficient transduction of human monocyte-derived dendritic cells with subgroup B fiber-modified adenovirus vectors enhances transgene-encoded antigen presentation to cytotoxic T cells. J. Immunol. 166, 5236–5244.

Reimann, K.A., Li, J.T., Voss, G., Lekutis, C., Tenner-Racz, K., Racz, P., Lin, W., Montefiori, D.C., Lee-Parritz, D.E., Lu, Y., Collman, R.G., Sodroski, J., Letvin, N.L., 1996. An *env* gene derived from a primary human immunodeficiency virus type 1 isolate confers high in vivo replicative capacity to a chimeric simian/human immunodeficiency virus in rhesus monkeys. J. Virol. 70, 3198–3206.

Roberts, D.M., Nanda, A., Havenga, M.J., Abbink, P., Lynch, D.M., Ewald, B.A., Liu, J., Thorner, A.R., Swanson, P.E., Gorgone, D.A., Lifton, M.A., Lemckert, A.A., Holterman, L., Chen, B., Dilraj, A., Carville, A., Mansfield, K.G., Goudsmit, J., Barouch, D.H., 2006. Hexon-chimaeric adenovirus serotype 5 vectors circumvent pre-existing anti-vector immunity. Nature 441, 239–243.

Sasaki, Y., Ami, Y., Nakasone, T., Shinohara, K., Takahashi, E., Ando, S., Someya, K., Suzaki, Y., Honda, M., 2002. Induction of CD95 ligand expression on T lymphocytes and B lymphocytes and its contribution to apoptosis of CD95-upregulated $CD4^+$ T lymphocytes in macaques by infection with a pathogenic simian/human immunodeficiency virus. Clin. Exp. Immunol. 122, 381–389.

Segerman, A., Mei, Y.F., Wadell, G., 2000. Adenovirus types 11p and 35p show high binding efficiencies for committed hematopoietic cell lines and are infective to these cell lines. J. Virol. 74, 1457–1467.

Shayakhmetov, D.M., Papayannopoulou, T., Stamatoyannopoulos, G., Lieber, A., 2000. Efficient gene transfer into human CD34 (+) cells by a retargeted adenovirus vector. J. Virol. 74, 2567–2583.

Shinohara, K., Sakai, K., Ando, S., Ami, Y., Yoshino, N., Takahashi, E., Someya, K., Suzaki, Y., Nakasone, T., Sasaki, Y., Kaizu, M., Lu, Y., Honda, M., 1998. A highly pathogenic simian/human immunodeficiency virus with genetic changes in cynomolgus monkeys. J. Gen. Virol. 80 (Pt. 5), 1231–1240.

Shiver, J.W., Fu, T.M., Chen, L., Casimiro, D.R., Davies, M.E., Evans, R.K., Zhang, Z.Q., Simon, A.J., Trigona, W.L., Dubey, S.A., Huang, L., Harris, V.A., Long, R.S., Liang, X., Handt, L., Schleif, W.A., Zhu, L., Freed, D.C., Persaud, N.V., Guan, L., Punt, K.S., Tang, A., Chen, M., Wilson, K.A., Collins, K.B., Heidecker, G.J., Fernandez, V.R., Perry, H.C., Joyce, J.G., Grimm, K.M., Cook, J.C., Keller, P.M., Kresock, D.S., Mach, H., Troutman, R.D., Isopi, L.A., Williams, D.M., Xu, Z., Bohannon, K.E., Volkin, D.B., Montefiori, D.C., Miura, A., Krivulka, G.R., Lifton, M.A., Kuroda, M.J., Schmitz, J.E., Letvin, N.L., Caulfield, M.J., Bett, A.J., Youil, R., Kaslow, D.C., Emini, E.A., 2002. Replication-incompetent adenoviral vaccine vector elicits effective anti-immunodeficiency-virus immunity. Nature 415, 331–335.

Someya, K., Xin, K.Q., Matsuo, K., Okuda, K., Yamamoto, N., Honda, M., 2004. A consecutive priming-boosting vaccination of mice with simian immunodeficiency virus (SIV) gag/pol DNA and recombinant vaccinia virus strain Dls elicits effective anti-SIV immunity. J. Virol. 78, 9842–9853.

Someya, K., Cecilia, D., Ami, Y., Nakasone, T., Matsuo, K., Burda, S., Yamamoto, H., Yoshino, N., Kaizu, M., Ando, S., Okuda, K., Zolla-Pazner, S., Yamazaki, S., Yamamoto, N., Honda, M., 2005. Vaccination of rhesus macaques with recombinant Mycobacterium bovis bacillus Calmette–Guérin Env V3 elicits neutralizing antibody-mediated protection against simian–human immunodeficiency virus with a homologous but not a heterologous V3 motif. J. Virol. 79, 1452–1462.

Someya, K., Ami, Y., Nakasone, T., Izumi, Y., Matsuo, K., Horibata, S., Xin, K.Q., Yamamoto, H., Okuda, K., Yamamoto, N., Honda, M., 2006. Induction of effective cellular and humoral immune responses by a prime-boost vaccine encoded with simian immunodeficiency virus gag/pol. J. Immunol. 176, 1784–1795.

Vogels, R., Zuijdgeest, D., van Rijnsoever, R., Hartkoorn, E., Damen, I., de Bethune, M.P., Kostense, S., Penders, G., Helmus, N., Koudstaal, W., Cecchini, M., Wetterwald, A., Sprangers, M., Lemckert, A., Ophorst, O., Koel, B., van Meerendonk, M., Quax, P., Panitti, L., Grimbergen, J., Bout, A., Goudsmit, J., Havenga, M., 2003. Replication-deficient human adenovirus type 35 vectors for gene transfer and vaccination: efficient human cell infection and bypass of preexisting adenovirus immunity. J. Virol. 77, 8263–8271.

Xin, K.Q., Jounai, N., Someya, K., Honma, K., Mizuguchi, H., Naganawa, S., Kitamura, K., Hayakawa, T., Saha, S., Takeshita, F., Okuda, K., Honda, M., Klinman, D.M., Okuda, K., 2005. Prime-boost vaccination with plasmid DNA and a chimeric adenovirus type 5 vector with type 35 fiber induces protective immunity against HIV. Gene Ther. 12, 1769–1777.

Xin, K.Q., Sekimoto, Y., Takahashi, T., Mizuguchi, H., Ichino, M., Yoshida, A., Okuda, K., 2007. Chimeric adenovirus 5/35 vector containing the clade C HIV *gag* gene induces a cross-reactive immune response against HIV. Vaccine 25, 3809–3815.

Yoshino, N., Ami, Y., Terao, K., Tashiro, F., Honda, M., 2000. Upgrading of flow cytometric analysis for absolute counts, cytokines and other antigenic molecules of cynomolgus monkeys (*Macaca fascicularis*) by using anti-human cross-reactive antibodies. Exp. Anim. 49, 97–110.